8-2022

Genomic Analysis and Characterization of Surface Properties of Naphthalene Degrading Acinetobacter Isolates

Gunn Emilie Berge

THE UNIVERSITY OF SOUTH ALABAMA
COLLEGE OF ARTS AND SCIENCES
SCHOOL OF MARINE AND ENVIRONMENTAL SCIENCES

GENOMIC ANALYSIS AND CHARACTERIZATION OF SURFACE PROPERTIES OF NAPHTHALENE DEGRADING *ACINETOBACTER* ISOLATES

BY

Gunn Emilie Berge

A Thesis

Submitted to the Graduate Faculty of the
University of South Alabama
in partial fulfillment of the
requirements for the degree of

Master of Science

in

Environmental Toxicology

August 2022

Approved:	Date:
Sinéad M. Ní Chadhain	24/6/2022
Chair of Thesis Committee: Dr. Sinéad M. Ní Chadhain	
	6-24-2022
Committee Member: Dr. David. C. Forbes	
Loren A. Launen	6-24-2022
Committee Member: Dr. Loren. A. Launen	
	06-27-2022
Program Coordinator: Dr. Alison Robertson	
	6/27/2022
Director of Graduate Studies: Dr. Eric Loomis	
Harold Pardue	7/14/2022
Dean of the Graduate School: Dr. J. Harold Pardue	

GENOMIC ANALYSIS AND CHARACTERIZATION OF SURFACE PROPERTIES OF NAPHTHALENE DEGRADING *ACINETOBACTER* ISOLATES

A Thesis

Submitted to the Graduate Faculty of the
University of South Alabama
in partial fulfillment of the
requirements for the degree of

Master of Science

in

Environmental Toxicology

by
Gunn Emilie Berge
B.S., University of South Alabama, 2020
August 2022

ACKNOWLEDGEMENTS

First and foremost, I would like to thank my mentor Dr. Ní Chadhain for the continuous support throughout the master's program, for her patience, encouraging words, and immense knowledge. Thank you for challenging me yet providing guidance when I needed it. I am forever grateful for all the feedback I have received while writing this thesis. My completion of this thesis would not have been accomplished without your support. I could not have asked for a better advisor and more committed mentor. Besides my mentor, I would like to thank the rest of my thesis committee: Dr. Forbes and Dr. Launen, for their encouragement and helpful feedback on laboratory procedures. I would like to thank Dr. Forbes, for letting me use his laboratory and for making me feel welcome. I would like to thank Dr. Launen for helping me sequence the genomes of some of my *Acinetobacter* isolates. I am truly grateful. I would also like to thank Dr. Robertson for being a great role model. Your compassion and work ethic are unmatched. Last, but not least, I would like to thank my family and friends. Your encouraging words have motivated me to work harder, and I am so grateful for the support at my thesis defense. A special thanks to my beloved husband for being my rock through the ups and downs. To everyone else who has helped me these last two years, thank you so much.

TABLE OF CONTENTS

Page

LIST OF TABLES

LIST OF FIGURES

LIST OF ABBREVIATIONS

BATH	Bacterial Adhesion to Hydrocarbons
BP	Biphenyl
E_{24} test	Emulsification Activity Assay
GC-MS	Gas Chromatography Mass Spectrometry
HGT	Horizontal gene transfer
MSA-N-I	Minimal salts agar containing indole and naphthalene
MSB	Minimal salts broth
MSBT-N	Minimal salts broth containing tryptic soy broth and naphthalene
MSMY-NIC	Minimal salts media containing yeast extract, naphthalene, indole, and cycloheximide
NP	Naphthalene
OD_{600}	Optical density at 600 nm
PH	Phenanthrene
RASTtk	Rapid annotations using Subsystem Technology toolkit
RHD	Ring hydroxylating dioxygenase
TSB	Tryptic soy broth

ABSTRACT

Berge, Gunn, Emilie M. S., University of South Alabama, August 2022. **GENOMIC ANALYSIS AND CHARACTERIZATION OF SURFACE PROPERTIES OF NAPHTHALENE DEGRADING *ACINETOBACTER* ISOLATES**. Chair of Committee: Sinéad M. Ní Chadhain, Ph.D.

Polycyclic aromatic hydrocarbons (PAHs) occur naturally in coal and crude oil. They also are produced from anthropogenic activities such as burning of coal, oil, and gas. PAHs accumulate in nature and can cause serious health problems. In this study, naphthalene-degrading bacteria were isolated from a naphthalene enrichment culture established from urban soil in Mobile, AL. Degraders were identified by their ability to grow on naphthalene and by the production of indigo from indole, a characteristic of naphthalene dioxygenase enzymes. Thirty-two isolates were identified by sequencing of the 16S rRNA gene. Ten isolates matching *Acinetobacter seifertii, Acinetobacter pittii, Acinetobacter baumannii,* and *Rhodococcus agglutinans* were selected for further study. All ten isolates grew on naphthalene, biphenyl and phenanthrene. Gas chromatography mass spectrometry was used to quantify and verify the removal of naphthalene. Emulsification and BATH assays were conducted to screen for biosurfactant production, which all ten isolates were found to produce. PAH catabolic genes were identified in the genomes of nine isolates. However, RT-PCR analysis of PAH-degradation gene expression was inconclusive. This study expands our knowledge of PAH degradation by *Acinetobacter*, a genus better known as opportunistic human pathogens.

CHAPTER I

BACKGROUND

1.1 Introduction

Polycyclic aromatic hydrocarbons (PAHs) are fused benzene rings that are ubiquitous in the environment. Some are released naturally by for example volcanic activities, but the majority are released via fossil fuel combustion and other anthropogenic activities (Abdel-Shafy and Mansour 2016). Hundreds of PAHs exist, and many are highly toxic in high concentrations or when part of certain mixtures. Studies show that PAHs can, among other things, cause birth defects and skin rashes (Rengarajan *et al.* 2015). Occupational, epidemiological, and animal studies have found that PAHs are potent mutagens and/or carcinogens and need to be considered hazardous to humans. The full effect will depend on factors such as duration and route of exposure, the volume or concentration of PAHs to which one is exposed, and the relative toxicity (Mallah *et al.* 2022). This study focuses on isolating and characterizing bacteria that can degrade PAHs.

1.2 Structure and Adverse Effects of PAHs

High molecular weight (HMW) PAHs with more than four benzene rings are especially carcinogenic. PAHs must be metabolically activated to cause carcinogenic effects and various enzymes can convert PAHs to metabolically active metabolites such

as electrophilic and redox-active metabolites (Jacob 1996). If DNA adducts are not repaired, they can cause cancer when they bypass error prone translesional DNA synthesis during cell replication. PAHs, along with PAH derivatives, can also promote cancer through non-genotoxic mechanisms (Murray and Penning 2018). PAHs are difficult to break down due to highly stable resonance structures with delocalized electrons which can lead to accumulation of PAHs in the environment compartments. High molecular weight PAHs are especially challenging to degrade (Patel *et al*. 2020). Although hundreds of PAHs exist, sixteen have been identified as high priority pollutants by the United States Environmental Protection Agency (USEPA) (**Figure 1**). These are all of great concern due to their hydrophobicity, mutagenicity, and toxicity to humans and nature and are studied more in-depth than other PAHs (Hussar *et al*. 2012).

1.3 Accumulation of PAHs in the Environment

PAHs are prevalent in marine and costal environments and harm many organisms. Large amounts of PAHs are released into the marine environment through anthropogenic oil spills and underground and above ground storage tank leaks (Abdel-Shafy and Mansour 2016). Surface soils (origin of bacteria in this study) and sediments continuously receive PAHs through atmospheric wet or dry deposition. For example, from local sources like automobile exhaust or distant sources through the air. Other sources include input from storm and sewer effluents, roadway runoff, and potentially PAH containing fill materials. Once PAHs are deposited into the ocean and or terrestrial systems, they can become mobile. On land, PAHs bind to soil particles and their mobility will highly depend on sorbent particle size, the pore throat size of the soils as well as soil

conductivity. The octanol–water partitioning coefficient of PAHs will also influence the binding of PAHs to soils (Abdel-Shafy and Mansour 2016).

As a result of the binding affinity to other matter, PAHs can easily be transported great distances. PAHs are resistant to degradation and do not mix well with water leading to bioaccumulate of PAHs in marine food webs. This accumulation of PAHs harms both the biological system itself and humans that consume PAH-contaminated seafood (Lee *et al.* 2018). Bioaccumulation of PAHs in terrestrial invertebrates is well documented, but degradation of PAHs is sufficient to prevent biomagnifications (Abdel-Shafy and Mansour 2016).

Liu *et al*. (2017) explored the abundance of 16 priority PAHs throughout the Pearl River Delta in China. They assessed their response to the seasonal variation of anthropogenic activities and hydrological cycles. The PAH concentration was higher during the wet season due to increased riverine discharge and atmospheric deposit. The suspended sediment concentration (SSC) was also higher during the wet season contributing to a higher concentration of the PAHs in suspended particulate matter (SPM) while higher temperatures and lower salinities contributed to desorption from SPM (Liu *et al.* 2017). Due to solubility differences, the low molecular weight (LMW) PAHs are more readily desorbed from SPM into the water than HMW PAHs (Giuliani *et al*. 2008). More than 62 PAHs were identified throughout the water column and the mean concentration of PAHs was higher during ebb tide than flood tide indicating an overall movement towards the ocean (Liu *et al*. 2014).

1.4 Remediation Strategies

PAHs can be removed by several remediation strategies: either by physical/chemical means, bioremediation, photooxidation, or leaching. All PAHs will react to these strategies in a different way as they all have a unique structure and a set of physical, chemical, and biological properties (Abdel-Shafy and Mansour 2016; Patel *et al*. 2020).

1.4.1 Physical/chemical Remediation Strategies

Common physical/chemical remediation strategies include membrane filtration, coagulation, advanced oxidation process, and adsorption. PAHs are chemically challenging to degrade as they are thermostable and display a high level of resonance stability and hydrophobicity (Patel *et al*. 2020). Mojiri *et al*. (2019) found that advanced oxidation procedures and electrooxidation techniques resulted in a 90.0-95.0% PAH removal efficiency. Other efficient methods were modified coagulation and membrane filtration with 90% or greater removal efficiency. Despite being efficient, most physical/chemical remediation strategies have strict operation conditions, high energy consumption, and expensive equipment (Mojiri *et al.* 2019).

1.4.2 Bioremediation

Bioremediation is an environmentally friendly strategy that utilizes various organisms already present in the environment to remove toxic PAHs *in situ* (Ma *et al.* 2021). *Ex situ* bioremediation involves the physical removal of polluted material by transporting it to another location, often to the area of treatment (Shah 2014). Plants, fungi, and bacteria have all been employed in the bioremediation of PAH in soil. These

organisms can break down PAHs and utilize them as a carbon and energy source (Ma *et al.* 2021). Some oxidize PAHs completely to carbon dioxide while others only break them down partway. Bioremediation is a highly promising strategy as it is inexpensive and does not require disruption of the natural and essential environments (Ghosal *et al.* 2016).

Natural attenuation, bioaugmentation, and biostimulation are the most frequently employed bioremediation strategies (33%). Natural attenuation involves improving PAH metabolism by simply optimizing aeration, moisture, and nutrient levels (Chikere *et al.*, Fubara 2017). Biostimulation focuses on enhancing bacterial growth and ultimately PAH degradation by adding different combinations of micro and macro nutrients (Patel *et al*. 2020). Finally, bioaugmentation involves adding competent PAH degrading bacterial strains or consortia of microorganisms. This improves degradation and may even enhance the catabolic capabilities of indigenous microorganisms. However, this strategy is highly unpredictable (Kong *et al*. 2018; Patel *et al*. 2020).

Another strategy is the microbial enzyme mediated bioremediation. This is a very efficient and selective strategy as it isolates target enzymes that can catalyze reactions at a wide range of PH levels and temperatures. Enzymes from fungi are especially efficient as they are less substrate specific. However, the isolation of selected enzymes is an expensive process (Kuppusamy *et al.* 2017). In addition to Mycoremediation, phytoremediation is also used as a bioremediation strategy to remove PAHs or convert them to less hazardous compounds (Patel *et al*. 2020). PAHs need to be bioavailable in order to be metabolized. PAHs that are bound to soil particles cannot easily be accessed as the compounds are separated from the enzymes needed to break down the benzene

rings (Wang *et al.* 2009). Cornelissen *et al.* (1998) found that the possible PAH degradation could be estimated from the initial rapidly desorbing fraction (Cornelissen *et al*. 1998). Age of the PAHs has been found to also affect bioavailability as older PAHs take longer to desorb from the soil than more recently added PAHs (Hatzinger and Alexander 1995). Another important factor is the water solubility. HMW PAHs are usually less soluble than LMW PAHs making them less bioavailable (Wang *et al.* 2009). PAH degradation can become inefficient by competitive inhibition. This happens when the active sites of catabolic enzymes are non-specific. Then, if compounds that require less energy to degrade are available, the enzyme will favor them over PAHs (Abdel-Shafy and Mansour 2016).

1.4.2.1 Mycoremediation.

Mycoremediation, which is bioremediation by fungi, is efficient at removing PAHs. Fungi can degrade a wide variety of PAHs. They produce extracellular enzymes such as lignin-degrading enzymes which break down and mineralize even high molecular weight PAHs. The most challenging and energy-demanding step in degrading PAHs is the initial step. Once the stable resonance structure is disrupted the PAHs loses its aromatic character and becomes easier to further break down (Shankhwar and Paliwal 2021). Fungi are more likely than bacteria to make the initial attach on PAHs as they possess extracellular enzymes, such as manganese peroxidase (MnP) and lignin peroxidase (LiP), that can diffuse to immobile PAHs. Thus, fungi can partially degrade PAHs to less hazardous intermediates such as oxo-ferryl and quinines which can be utilized by other microorganisms such as bacteria (Peng *et al.* 2008).

Earlier studies reported that both ligninolytic and non-ligninolytic fungi can degrade PAHs with oxidation being the first step. Ligninolytic fungi use enzymes such as manganese peroxidase (MnP), lignin peroxidase (LiP), and laccase to convert PAHs to quinone intermediates. Non-ligninolytic fungi, on the other hand, can utilize intracellular cytochrome P450 monooxygenases which are known for their ability to catalyze the insertion of oxygen into various compounds. Non-ligninolytic fungi and some ligninolytic fungi have been described to possess cytochrome P450 monooxygenases /epoxide hydrolase which catalyze the reaction that forms trans-dihydrodiols (Mueller *et al.* 1995). Cytochrome P450 can also oxidize PAHs to phenols which go on to be conjugated with sulfate, glucoronic acid, or glucose (Cerniglia *et al*. 1982; Casillas *et al*. 1996; Pothuluri *et al*. 1996).

Park *et al*. (2019) described the genomic and transcriptomic analysis of PAH degradation by the white-rot fungus *Dentipellis* sp. This fungus displayed the classical wood decay mode and could efficiently degrade and remove (>90% of 100 ppm PAH) phenanthrene, anthracene, fluoranthene, and pyrene. Transcriptomic analysis revealed 1922 genes upregulated in the presence of at least one of these PAHs. It also revealed 11 genes encoding ligninolytic enzymes, which are thought to be the key in PAH removal, along with some non-ligninolytic enzymes. Interestingly, *Dentipellis* sp. efficiently removed PAHs without upregulating any significant ligninolytic genes. They believe that P450s mediate the first oxidation step of aromatic rings as they were highly upregulated (Park *et al.* 2019).

Phanerochaete chrysosporium have been found to oxidize pyrene, anthracene, fluorene, and benzo[α]pyrene using the enzymes lignin peroxidase and manganese

peroxidase (Peng *et al.* 2008). Ma *et al.* (2021) used *Crucibulum laeve,* which is a common bird's nest fungi, to assess its ability to degrade PAHs. Over 60 days *Crucibulum laeve* significantly reduced the concentration of pyrene, phenanthrene, and benzo(a)pyrene in soil. Pyrene was reduced from 2600 μg kg^{-1} to 1500 μg kg^{-1}, phenanthrene from 2200 μg kg^{-1} to 750 μg $kg^{-1,}$ and benzo(a)pyrene from 1400 μg kg^{-1} to 800 μg kg^{-1}.

1.4.2.2 Bioremediation by Bacteria.

Bacteria degrade PAHs faster than fungi and are important players in removing hydrocarbons after oil spills (Lee *et al.* 2018). A variety of bacteria have been documented to metabolize and degrade LMW and HMW PAHs in nature. The best or most complete PAH degradation is usually achieved by a mixture of different bacteria as a result of collaborative catabolic activities. Bacteria possess different catabolic enzymes and will likely utilize a variety of PAH degradation pathways and form intermediates that can be further metabolized or mineralized by other strains (Vaidya *et al.* 2018; Haleyur *et al.* 2019).

One major obstacle of bioaugmentation in soil/sediments is a dispersion of inoculum. It is particularly difficult in subsurface soil due to little microbial transport as cells easily adhere to soil organic matter. Immobilized *Pseudomonas taiwanensis* PYR1 and *Acinetobacter baumannii* INP1 on cinder beads have been reported to increase pyrene and indeno[1,2,3-cd]pyrene degradation (71 and 81%). Immobilization offers biological stability, less competition with surrounding bacteria, and protection from harsh environmental conditions (Mrozik and Piotrowska-Seget 2010; Huang *et al.* 2016).

Extremophiles such as halophilic, acidophilic, and thermophilic bacteria have also been reported to remove PAHs. Bacteria with tolerance for high temperatures have an advantage as elevated temperatures enhance the bioavailability of PAHs by lowering their viscosity (Mehetre *et al*. 2019). A biostimulation experiment was conducted on PAH contaminated soil and the greatest bioactivity resulted from adding low levels of macronutrients and high levels of micronutrients. The nutrient solution (MS6) consisted of 75% sulfur, 3% nitrogen, and 11% phosphorus dry weight. Known PAH degraders were used, and the average total oxygen consumption after 72 hours was used to determine the effect of the biostimulation experiment. About 1600 µl of cumulative oxygen consumption was removed without the addition of nutrients (control) while over 3500 µl of oxygen was used in treatments with added nutrients suggesting increased bioactivity with added nutrients (Liebeg and Cutright 1999).

Another study assessed PAH degradation potential by collecting surface sediment samples from seven contaminated mangrove swamps in Hong Kong SAR. Samples were collected in triplicates from seven locations, namely Kei Ling Ha Lo Wai (KLH), Sai Keng (SK), Ho Chung (HC), Ma Wan (MW), Yi O (YO), Sheung Pak Nai (SPN) and Mai Po (MP). The samples were collected from the middle of the swamps during low tide. Bacteria were isolated by using PAH supplemented enrichment cultures. The samples enriched from Sai Keng and Ho Chung sediments performed the best, removing 90% of the phenanthrene and fluoranthene in seven days. According to 16S rDNA gene sequences, the identities of the isolates were *Rhodococcus* (HCCS), *Sphingomonas* (MWFG) and *Paracoccus* (SPNT). Note that both gram-positive and gram-negative PAH degrading bacteria were isolated (Guo *et al.* 2005).

Many bioremediation projects that focus on the removal of HMW PAHs find that they are more challenging to remove than LMW PAHs which has led to an increased focus on investigating a wide phylogenetic spectrum of organisms with the ability to degrade HMW PAHs (Wilson and Jones 1993). The highest-molecular weight PAHs that can be fully degraded and utilized as sole carbon and energy source are four ring PAHs, like pyrene and chrysene. The genera associated with this degradation are: *Rhodococcus* sp. (Walter *et al.* 1991), *Burkholderia cepacia* (Juhasz *et al.* 1996, 1997), *Stenotrophomonas maltophilia* (Boonchan *et al.* 1998), *Mycobacterium* sp. (Heitkamp *et al.* 1988; Kästner *et al*. 1994; Bouchez *et al*. 1995), *Alcaligenes denitrificans* (Weissenfels *et al*. 1990), and *Sphingomonas paucimobilis* (Ye *et al.* 1996). Some of these isolates can also degrade five membered rings partway. Again, both gram-positive and gram-negative bacteria have been documented to mineralize HMW PAHs.

The ideal PAH degrader to employ in a bioremediation project should have the ability to survive on PAHs as the sole carbon source. This is very important to avoid the production of more water-soluble and toxic by-products and intermediates and so that the bacterium will survive in harsh environments with few growth substrates present (Boonchan *et al*. 2000). As mentioned above, high molecular weight PAHs are especially difficult to degrade which is likely due to their high hydrophobicity and complex structure including numerous fused benzene rings (**Figure 1**). High molecular weight PAHs cannot get through the bacterial cell wall. Boonchan *et al.* (2000) found that the bacterium *S. maltophilia* VUN and the fungus *P. janthinellum* VUO are only able to survive with benzo[a]pyrene as the sole carbon and energy source when they are combined in fungal-bacterial cocultures. This indicates that complete mineralization of

benzo[a]pyrene requires metabolic activity and cooperation from both organisms (Boonchan *et al*. 2000).

Not all bacteria possess PAH degrading functional genes and most bacteria are unable to metabolize them. A comprehensive phylogenetic study investigated PAH degrading bacteria from various locations. This study found that PAH degradation is associate with specific genera regardless of their geographic location (Mueller *et al.* 1997). A similar phylogenetic study identified a shift in community structure towards gammaproteobacterial, from alpha- and betaproteobacteria, following expose to PAHs (Stoffels *et al.* 1998). Some of the best characterized PAH degrading bacteria include *Pseudomonas, Sphingomonas, Brevibacterium, Arthrobacter, Nocardioides,* and *Mycobacterium* (Lu *et al.* 2019).

1.4.2.3 Combined Bioremediation.

Soil consists of a diverse and complex ecosystem of various organismal interactions. Microbial communities are diverse and interactions among communities and between the various microorganisms can alter the function of the community. Ma *et al*. (2021) conducted a 60-day greenhouse pot experiment to explore and compare the PAH degradation abilities of mycoremediation (MR), phytoremediation (PR), natural attenuation (NA) and plant-microbial remediation (PMR). *Salix viminalis* (PR) and *Crucibulum laeve* (MR) are known PAH degraders and were selected for the experiment. Quantitative PCR of fungal rRNA internal transcribed spacer region (ITS) was uses to assess fungal biomass.

The hypervariable V3-V4 region of the bacterial16S rRNA gene and the fungal rRNA internal transcribed spacer (ITS) region was sent out for Illumina NovaSeq

sequencing. Quantitative PCR was conducted on the16S rDNA, ITS, and the PAH-RHDα GP gene. PICRUSt software predicted sixteen genes to be associated with PAH degradation by *C. laeve*. The most common and relevant genes associated with mycoremediation were salicylate hydroxylase (K00480) and 1,3,7-trimethyluric acid 5-monooxygenase (K00492) (Ma *et al.* 2021). In this study, PAH degradation by bacteria was the most efficient PAH removal process. However, plant stimulation negatively affected the microbial degradation of PAHs due to competition for nutrients. This was further supported by a declining 16S rRNA gene copy number under phytoremediation treatment. Of the four bioremediation treatments, plant-microbial remediation (PMR) achieved the highest removal of pyrene, phenanthrene and benzo(a)pyrene. Both MR and PR also reduced PAH levels. However, by comparing MR with PR it was determined that they complemented each other and performed better when combined as MR added nutrients while PR consumed them. Thus, combining mycoremediation with phytoremediation synergistically supports the growth of diverse PAH degrading bacteria and improves the removal of soil PAHs (Ma *et al.* 2021).

1.5 Common Bacterial PAH Degradation Pathways

Bacteria use a variety of strategies to break down structurally different PAHs. The most common pathways to overcome the intrinsic chemical stability of PAHs are the aerobic peripheral pathways. The first step in these pathways involves an attack by a ring hydroxylating dioxygenase (RHD) which hydroxylates the benzene ring with help of activated molecular oxygen. The reaction leads to (di)-hydroxylated intermediates which are further degraded to central intermediates such as such catechol, protocatechuate,

gentisate (2,5-dihydroxybenzoate), and homogentisate (2,5-dihydroxyphenylacetate). Although many different pathways and genes have been described, the PAH degradation pathways converge on the same central intermediates. The central intermediates are 'activated' for oxidative ring cleavage, due to their electron-rich substituents in the ortho or para position (**Figure 2**). The structures can be cleaved by intradiol or extradiol ring-cleaving dioxygenases through either an ortho-cleavage pathway (between the two hydroxyl groups) or a meta-cleavage pathway (adjacent to the hydroxyl groups).

If cleaved by intradiol ring-cleaving dioxygenases, catechol and protocatechuate are converted to β-ketoadipate through the β -ketoadipate pathway. β-ketoadipate can further be converted to tricarboxylic acid cycle intermediates. If cleaved by extradiol ring-cleaving dioxygenases through meta-cleavage pathway, then catechol and protocatechuate are converted to acetaldehyde and pyruvate, respectively (**Figure 3**). PAH-ring hydroxylating dioxygenase (RHD) genes are functional genes that code for enzymes that initiate PAH degradation. Bacteria might possess different RHD genes and will degrade some PAHs more efficiently than others (Cerniglia 1992; Eaton and Chapman 1992; Gibson and Parales 2000; Fuchs *et al*. 2011).

Another common strategy to cleave aromatic rings is the epoxidation of CoA thioesters. This also requires oxygen to form the highly reactive epoxide which is easily rearranged to form other compounds. Microorganisms that live under anoxic conditions utilize the anaerobic peripheral pathway. This process is demanding and requires a reducing agent with redox potential. Electron-withdrawing intermediates such as benzoyl-CoA are used by ring-reducing enzymes in the central pathway to help transfer

electrons to the ring (Fuchs *et al*. 2011). Anaerobic degradation is less described as it is not the focus of this study.

1.6 Genomic studies of PAH Degrading Bacteria

Dioxygenases that are known for creating *cis*-dihydrodiols are frequently discovered in bacteria. Because of their frequency in bacteria and similarities, studies have shown that dioxygenases can be utilized as biomarkers to assess PAH degradation potential in environmental samples (Resnick *et al.* 1995; Chikere and Fenibo 2018). However, PCR primers designed to target dioxygenases will not detect all PAH degraders in an environmental sample. One solution is to design primers that target certain subsets of PAH dioxygenase genes (Meyer *et al.* 1999; Widada *et al.* 2002).

Aromatic degrading enzymes are often classified based on the growth substrate. For example, toluene (TDO), naphthalene (NDO), and biphenyl (BPDO). The TDO system works best for *cis*-hydroxylation of substituted benzene rings. Larger and bulky compounds do not fit well with the active site of the enzyme. NP and BP catalyze dihydroxylation of larger PAHs (Boyd and Sheldrake 1998). The NP dioxygenase system is often used to oxidize bi- and tri- cyclic PAH substrates, such as naphthalene, phenanthrene and anthracene. The NP system is a multicomponent enzyme that usually involves a NADH oxidoreductase, a ferredoxin and an oxygenase component. NDO is composed of a large (alpha) and small (beta) subunit which contain a Rieske [2Fe–2S] center and mononuclear nonheme iron. The *nahAaAb* genes encode the ferredoxin and reductase components and are important for the transport of electrons and allow for

activation of molecular oxygen (Butler and Mason 1997; Parales *et al*. 1998; Laurie and Lloyd-Jones 1999).

The NP catabolic genes (*nah*) of NAH7 are arranged in two operons. The *nal* operon encodes the proteins in the upper pathway which converts NP to salicylate. The *sal* operon encodes the proteins in the lower pathway which converts salicylate to pyruvate and acetyl coenzyme A. The pathways are genetically linked and regulated by the gene, *nah*R (Yen and Gunsalus 1982; Grund and Gunsalus 1983). The proteins in the upper pathway that are responsible for converting naphthalene to salicylate have also been found to convert phenanthrene to naphthalene-1,2-diol (Laurie and Lloyd-Jones 1999).

Genes encoding the upper pathway proteins have been documented for many bacterial strains: *ndo* genes were reported from *Pseudomonas putida* NCIB 9816 (Yang *et al*. 1994), *nah* genes from *P. putida* G7 (Menn *et al*. 1993), *dox* genes from *Pseudomonas* sp.C18 (Denome *et al.* 1993), *pah* genes from *P. putida* OUS82 (Kiyohara *et al.* 1994) and *Pseudomonas aeruginosa* Pak1 (Takizawa *et al.* 1999), and *nah* genes from *Pseudomonas stutzeri* AN10 (Bosch *et al*. 1999).

The proteins in the upper pathways are very similar (>90 % amino acid identity) and are arranged similarly. Enzymes identified in *Pseudomonas* strains are: *nahAa* (ferredoxin reductase), *nahAb* (NDO ferredoxin), *nahAc* (the α -subunit of NDO), *nahAd* (the β -subunit of NDO), naphthalene *cis*-dihydrodiol dehydrogenase (nahB), salicylaldehyde dehydrogenase (*nahF*), 1,2-dihydroxynaphthalene dioxygenase (*nahC*), trans-o-hydroxybenzylidenepyruvate hydratase-aldolase (*nahE*), and 2-hydroxychromene-2-carboxylateisomerase (*nahD*). This study also identified *ndo* genes

from *P. putida* strain NCIB9816 (M23914), *dox* genes from *Pseudomonas* sp. strain C18 (M60405), *pah* genes from *P. aeruginosa* strain PaK1 (D84146), and *pah* genes from *P. putida* strain OUS8247 (AB004059) (Habe and Omori 2003).

Genome analysis cannot always explain observed PAH-degradation phenotypes indicating that novel PAH degradation genes and pathways may exist. Lloyd *et al.* (1999) found that 45 % (20/44) of bacteria with a NP-degrading phenotype can be monitored by a *nah*A*c* probe (from *Pseudomonas putida* G7). Analogues of the bacterial glutathione S-transferase (GST) encoding gene (from *Sphingomonas paucimobilis* EPA505) have been linked to phenanthrene-degradation and hybridized to 29 % (10/35) of the isolated phenanthrene-degrading bacteria. Lastly, the *phn*Ac gene was not detected in any of the cultured isolates, except for the *Burkholderia* host strain (Lloyd-Jones *et al.* 1999).

Cycloclasticus sp. strain A5 is an obligate marine bacterium and was found to break down naphthalene, dibenzothiophenes, phenanthrenes, and fluorenes. Genomic analysis revealed 10 open reading frames, seven of which displayed homology to other characterized genes involved in PAH degradation. These functional genes are called *phn* genes and are commonly found in *Burkholderia* isolates. The first four, *phnA1, phnA2, phnA2, and phnA1,* were identified as PAH dioxygenase genes (Laurie and Lloyd-Jones 1999; Kasai *et al*. 2003).

Naphthalene dioxygenase activity in multiple *Pseudomonas* isolates that could completely degrade naphthalene was assessed by monitoring the NP degrading gene (*nahAc).* Interestingly, when grown on naphthalene, elevated levels of *nahAc* transcripts were recorded for *Pseudomonas monteilii* P26 and *Pseudomonas stutzeri* N3 and not for

Pseudomonas xanthomarina N12 suggesting that other novel genes are present or that the genes are always transcribed (Isaac *et al.* 2015).

A similar study investigated the frequency of the naphthalene dioxygenase gene (*nahAc*) in bacteria isolated from two illegally used modular refining sites in Nigeria. Using PCR, the *nahAc* gene was also detected in the genera of *Enterobacter, Pseudomonas, Burkholderia, Bacillus, Acinetobacter, Exiguobacterium* and *Stenotrophomonas* (Chikere and Fenibo 2018).

1.7 PAH Degradation by *Acinetobacter*

Acinetobacter isolates are Gram-negative, non-motile, aerobic bacteria known for their ability to survive in challenging environments such as hospitals. *Acinetobacter* isolates are resistant to most antimicrobial agents and can cause several infections, such as hospital acquired pneumonia. *Acinetobacter baumannii* is frequently responsible for nosocomial infections. Production of biofilm contributes to their colonization at hospitals and enhances their pathogenicity (Eze *et al*. 2018).

Previous research has described PAH degradation by *Acinetobacter* strains, but the phenomenon is not as well described as in other Gram-negative genera. Little genetic information is available on PAH degradation genes from *Acinetobacter* species. *Acinetobacter* sp. WSD, isolated from a coal-mining area, could use fluorene, phenanthrene and pyrene as the sole energy source. Approximately 90% of fluorene and phenanthrene were removed and 50% of pyrene was removed after six days of incubation (Shao *et al*. 2015).

Czarny *et al.* (2020) tested the theory that a microbial community isolated from a PAH and heavy metal contaminated location should exhibit a high bioactivity and biodegradation efficiency, despite decreased biodiversity resulting from harsh environment. *Acinetobacter, Pseudomonas, Stenotrophomonas* and *Achromobacter* were the dominant bacteria genera identified in this study. *Acinetobacter* was found to increase in abundance in environments with PAHs and heavy metals and outcompeted the other genera. This implies that the *Acinetobacter* genus is resilient to such contaminants and may be a dominant genus in soil populations exposed to mixed contminants (Czarny *et al.* 2020).

Bacteria normally carry a negative charge on the cell surface and to modify their cell surface properties or produce surfactants in order to take up hydrophobic compounds such as medium- and long-chain-length n-alkanes, and PAHs (Rojo 2009). *Acinetobacter baumannii* BJ, isolated from petroleum oil contaminated soil, was found to metabolize a maximum of 336 ppm of pyrene in 14 days ($C_{initial}$ = 600 ppm). Part of this enhanced pyrene removal was credited to *A. baumannii* BJ's ability to produce glycolipid biosurfactants. The cationic biosurfactants helps to provide surface and availability to the bacteria (Gupta *et al.* 2020). Other *Acinetobacter* isolates have been documented to produce biosurfactants. For example, Zhou *et al.* (2020) identified *Acinetobacter* strain Y2 which was found to produce biosurfactants, could reduce surface tension, and significantly enhanced PAH removal (Zhou *et al.* 2020).

Acinetobacter is not one of the most common PAH degradation genera, but *Acinetobacter* isolates have been found to efficiently degrade petroleum crude oil (PCO) (1.0 % v/v). C8 alkane hydrocarbons were degraded upon the addition of glucose (69.69

%) and the bacterium could degrade up to C14 alkane hydrocarbons when yeast extract was added. Thus, *Acinetobacter* can assist in the degradation of PCO following an oil spill especially with the addition of glucose and yeast (Goveas and Sajankila 2020).

Simarro *et al*. (2012) assessed PAH degradation abilities by conducting growth assays on two environmental samples. One was collected from heavily petroleum polluted soil (C2PL05) and the other was collected from decomposing wood in an unpolluted forest (BOS08). The effect of temperature, 5-15 °C versus 15-25 °C, on degradation rate was also investigated. For C2PL05, the temperature caused a significant difference in PAH removal, with higher values at increased temperatures. Temperature did not appear to cause a difference in PAH removal by the BOS08 consortium. The total PAH removal (pyrene, anthracene, perylene, and phenanthrene) was 98.9 % (SD ± 0.4) and 86.6 % (SD ± 6.0) for C2PL05 and BOS08, respectively at high temperatures. The total PAH removal was 54.3 % (SD ± 10.9) and 67.7 % (SD ± 7.7) for C2PL05 and BOS08, respectively at low temperatures. *Acinetobacter* spp. were identified in both samples (Simarro *et al*. 2012).

Ghosal *et al*. (2013) documented that *Acinetobacter* sp. strain AGAT-W, isolated from contaminated soil, could metabolize acenaphthene and acenaphthylene. The strain could survive using acenaphthene or acenaphthylene as the sole source of carbon. This was the first time these HMW PAHs had been reported to be mineralized by a strain belonging to the genus *Acinetobacter* (Ghosal *et al.* 2013).

Following genome analysis, an *Acinetobacter calcoaceticus* strain was found to encode a multicomponent oxygenase system (*benABC*) that catalyzed the conversion of benzoate to a nonaromatic *cis*-diol. Amino acid sequences of BenABC were compared to

the multicomponent system of toluate, toluene, benzene, and naphthalene 1,2-dioxygenases. The results indicated that the similarly sized subunits of the hydroxylate components may be derived from a common ancestor (Neidle *et al.* 1991).

Genome sequencing was also performed on *Acinetobacter venetianus* VE-C3 which is a described PAH degrader. Phylogenetic analysis revealed that it is likely distantly related to other *Acinetobacter* isolates. Genome analysis identified genes likely involved in the degradation of long chain n-alkanes and in the resistance to toxic metals, such as arsenic and cadmium. The genome contained multiple DNA mobilization-related genes suggesting the influence of horizontal gene transfer (HGT) in shaping the genome (Fondi *et al.* 2013).

Degradation experiments on various pollutants are conducted to assess degradation ability and efficiency. A bacterium capable of degrading diesel-oil and n-hexadecane was isolated from Deok-So, South Korea. DNA-DNA hybridization data indicated the discovery of a novel species and was named *Acinetobacter oleivorans* DR1^{T}. Strain DR1^{T} was an aerobic coccobacillus and grew best at 30°C with a pH of 6-8 (Kang *et al.* 2011). Kotoky *et al.* (2017) isolated *Acinetobacter* sp. PDB4 from petroleum contaminated soil and studied its ability to degrade benzo(a)pyrene (BaP), produce biofilm, and promote plant growth. The isolate had already shown ability to degrade LMW PAHs and HPLC and GC–MS analysis found that PDB4 removed 80.34% of BaP in 21 days of incubation. Strain PDB4 produced biofilm as a stress response upon addition of PAHs and increased PAH concentration lead to a greater release of glutathione-S-transferase. Finally, the strain displayed promising plant growth

characteristics such as the solubilization of phosphate *in vitro*, suggesting that it could be utilized in rhizoremediation projects (Kotoky *et al.* 2017).

1.8 This Study

In this study, I worked with the Fall 2020 BLY 314 class to isolate and characterize a collection of naphthalene degrading bacteria. Naphthalene is the simplest polycyclic aromatic hydrocarbon consisting of two fused benzene rings and is often used as a model compound for PAH degradation (**Figure 1**). My thesis research focuses on characterization of a subset of ten of these isolates. Growth by the selected isolates was quantified on naphthalene (NP), phenanthrene (PH), and biphenyl (BP). BATH assay and PAH-induced emulsification activity were quantified to investigate surface properties and production of biosurfactants by the isolates. Genome sequence information is provided for nine PAH degrading bacteria isolated during this study. The removal of naphthalene was quantified using a GC-MS and the function of a predicted PAH degradation gene was investigated using RT-PCR.

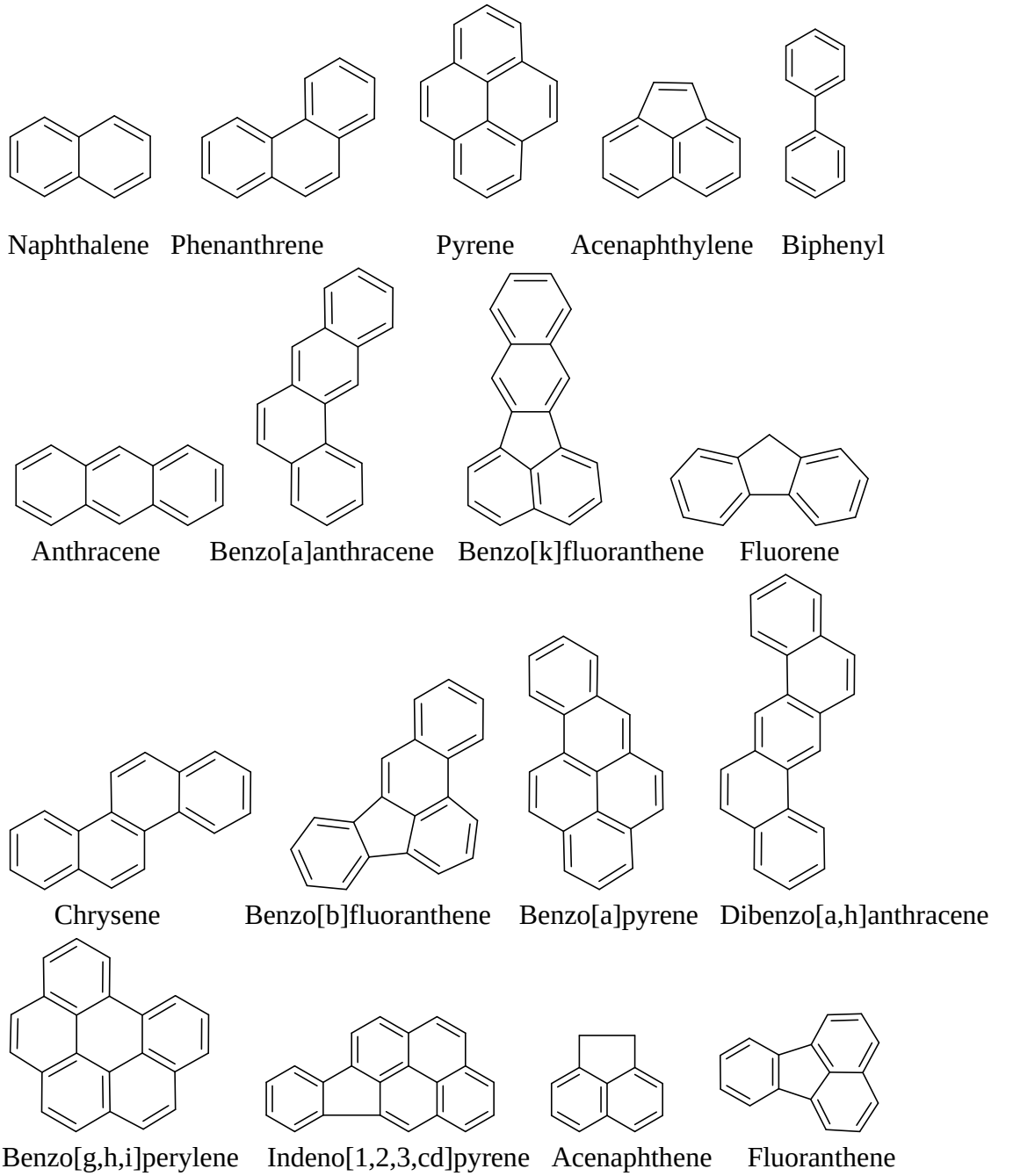

Figure 1. Chemical structure of 16 U.S. EPA priority pollutant PAH compounds (Rogers 2002) and biphenyl. Biphenyl is not a PAH but is often metabolized using the same biochemical pathway (Chen *et al.* 2021).

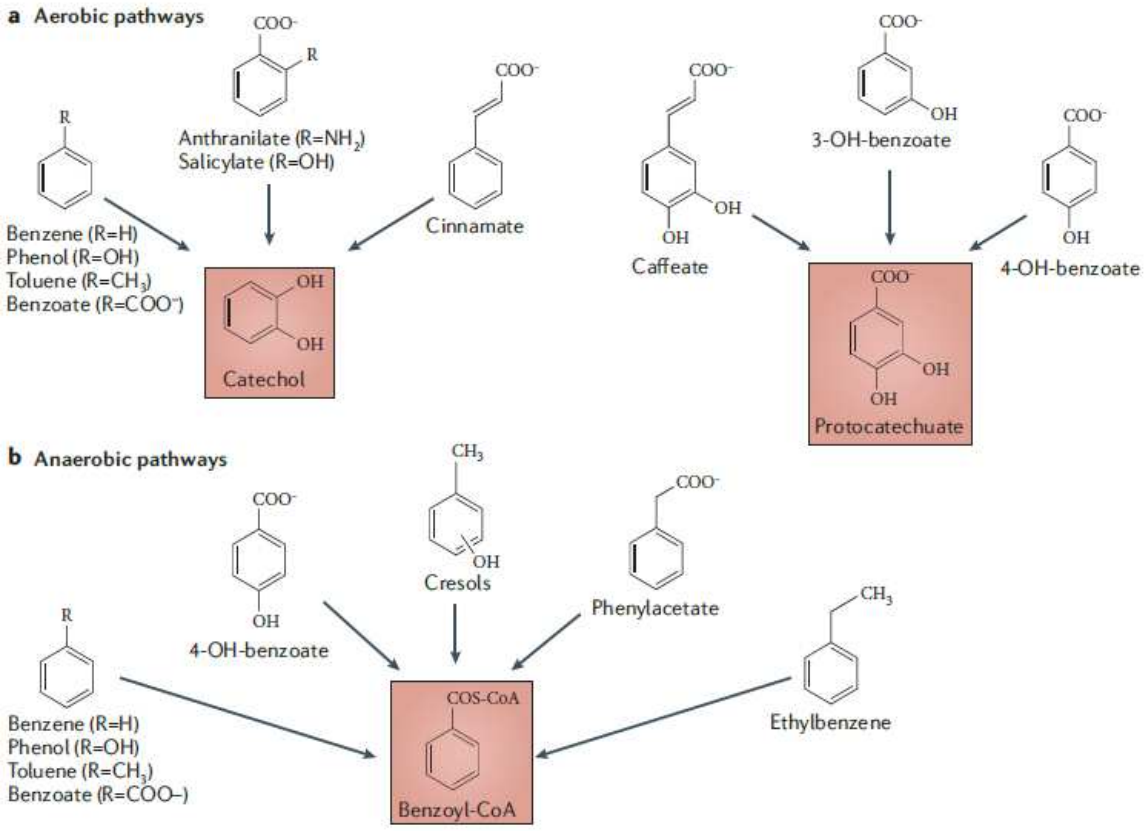

Figure 2. Aerobic (a) and anaerobic (b) aromatic hydrocarbon biodegradation pathways. Common central intermediates in the classical O_2 -dependent aerobic pathway are catechol and protocatechuate. These become substrates for ring-cleaving dioxygenases. The most common central intermediate for the anaerobic pathways is benzoyl-CoA which also becomes a substrate for ring-reducing enzymes (Fuchs *et al*. 2011).

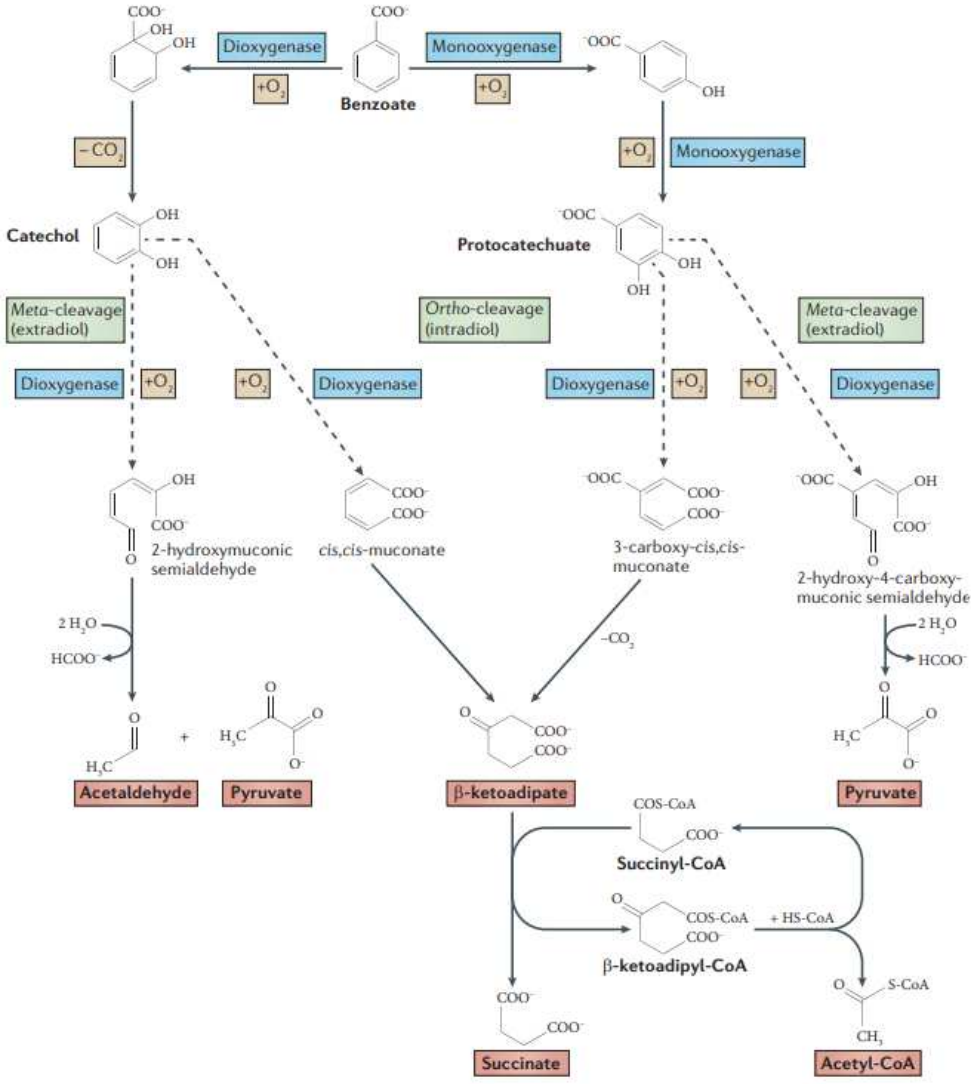

Figure 3. The classical O_2-dependent degradation pathway of benzoate in bacteria and fungi. Fungi convert benzoate to protocatechuate while most bacteria convert it to catechol. In the central pathway, ring-cleaving dioxygenases cleave the ring in the ortho-position (β-ketoadipate pathway) or the meta-position (Fuchs *et al*. 2011).

CHAPTER II

RESEARCH OBJECTIVES

The objectives of this study are:

- Isolate and identify naphthalene degrading bacteria from an urban soil sample.
- Characterize the PAH degradation range of the naphthalene degrading isolates.
- Quantify PAH degradation by the naphthalene degrading isolates.
- Characterize the surface characteristics and biosurfactant production of the naphthalene degrading isolates.
- Sequence and analyze the genomes of naphthalene degrading isolates.
- Identify and experimentally confirm the function of PAH degradation genes.

CHAPTER III

MATERIALS AND METHODS

3.1 Isolation and Purification of Naphthalene Degrading Bacteria

All culturing was performed using minimal salt medium (MSM) supplemented with naphthalene and indole. Per liter, media comprised of: 40 mL of Na_2HPO_4 + KH_2PO_4 buffer (M; pH 6.8); 20 mL of Hutner's vitamin-free mineral base and 1.0 g of $(NH_4)_2SO_4$ (Stanier *et al*. 1966). Soil samples were collected near a creosote-soaked wood telephone pole from midtown Mobile, AL. Enrichment cultures were prepared by inoculating 10 g of soil into 90 mL of mineral salt medium (10^{-1}) containing 1mM naphthalene and 75 μg mL^{-1} cycloheximide.

The enrichments were incubated for one week at room temperature and 200 rpm. The enrichments contained 10 mL MSB, 1 g soil and was stored in 100 mL capped serum bottles. Enrichments were further serial diluted to 10^{-9} and spread plated onto MSM-NP-Indole agars. Plates were incubated at room temperature for 24-48 hours before single colonies were transferred to fresh minimal salt medium containing 0.1% yeast extract, 0.5 mM naphthalene, 2 mM indole, and 75 μg mL^{-1} cycloheximide (MSMY-NIC). Some of the colonies were able to oxidize indole to indigo forming blue colonies. Conversion of indole to indigo is indicative of naphthalene dioxygenase activity, the first step in degrading many PAHs. This property has been found to be strongly induced by

naphthalene (Mercadal *et al*. 2010). Individual naphthalene degrading isolates were isolated by re-streaking single blue colonies onto minimal salt agar until the cultures appeared pure (MSA-NP-I). Single naphthalene degrading bacteria were transferred to test tubes containing tryptic soy broth (TSB) and incubated overnight at 200 rpm and 29 ºC. Freezing media (50% glycerol) in 1:1 ratio was added before storage at -80 ºC.

3.2 Microscopy and Morphological Tests

Negative, simple, and gram staining was performed to determine morphology and the phenotypic characterization of the isolates. A series of biochemical tests were performed to further characterize the isolates (Willey *et al.* 2008)

3.3 Identification of Naphthalene Degrading Bacteria

The 16S rRNA (primer set 27F and 1492R) and *pahE* genes (Hong Sunhee 2016; Liang *et al.* 2019) were amplified by polymerase chain reaction (PCR) using the colony touch method and GoTaq master mix according to manufacturer's guidelines (Promega, Madison, WI). The PCR program was set for 35 cycles with denaturation at 94 °C for 30 seconds, annealed at 55 °C for 30 seconds, and extension at 72 °C for 90 seconds, followed by 7 min at 72 °C, held at 12 °C. (Ausubel *et al*. 2002).

Gel electrophoresis was performed by preparing a 1% TAE agarose gel (Bio-Rad, Hercules, CA) (1h @ 100V) with SYBR Safe DNA gel stain (Invitrogen, Carlsbad, CA). Gel images were captured using a Bio-Rad Gel Doc^{tm} EZ imager image analysis system with Image Lab^{tm} (V3.0) software (Bio-Rad, Hercules, CA). The GeneRuler 100bp Plus

DNA ladder (Thermo Scíentific) was used to calculate the size of our PCR products and the expected size was ~1500 bp for 16S rRNA and ~370 bp for *pahE* (**Table 1**).

The *pahE* amplicons were not sent out for sequencing. The 16S rRNA gene was successfully amplified in all bacteria and sent out for sequencing to identify the isolates. BLASTn (Altschul *et al*. 1990) was used to identify the top BLAST matches from the GenBank database and determine homology.

3.4 Growth Assays

Single colonies of each isolate were aseptically inoculated into 5 mL MSB containing 100 ppm naphthalene (25mg mL^{-1} in 95% ethanol) and 10 µl tryptic soy broth (MSBT-N, Difco). Isolates were incubated overnight at room temperature and 200 rpm. The next day 100 µl was transferred to fresh media and grown for 24 hours at room temperature and 200 rpm. On the third day 0.5 mL of the overnight culture was inoculated into 25 mL of MSBT-N. Assays were carried out in triplicates. Microbial growth was determined using a Vernier spectrophotometer and Vernier Spectral Analysis software (Vernier) to measure OD at 600 nm (OD_{600}). The equipment was blanked with MSB solution containing naphthalene and TSB. Flasks were incubated at room temperature and 200 rpm. OD was measured by pipetting 1 mL of solution from each flask into a cuvette to read absorbance at 600 nm. Initial absorbance was recorded followed by reading every two hours for 14 hours with a final reading after 24 hours (**Figure 4**). The same procedure was used to measure bacterial growth on biphenyl and phenanthrene (Charan 2017) (**Figure 5** & **6**). Biphenyl, while not a PAH, was included

because it is frequently included in LMW PAH studies and has a well described degradation pathway (Roy 2013).

Control assays were performed to assess the role of TSB and ethanol in supporting isolate growth. The first control growth assay was done at 100 ppm NP. Previous growth assays contained supplemented TSB and so the first control growth assay was done to assess the influence of TSB (**Figure 7**). The second control growth assay contained 50 µl TSB and was set up to determine if the isolates were growing on TSB rather than on the tested PAH. Finally, the third control growth assay was performed with the 100 µl 95% ethanol (solvent) to verify that the isolates are growing on the PAHs and not the solvent (**Table 3** & **4**).

3.5 PAH Degradation Assays

Five hundred µl of overnight cultures, prepared in identical manner as growth assays, were aseptically transferred to 100 mL serum bottles containing 10 mL of MSB (Stanier, *et al*. 1966) and spiked with 100 ppm of NP. The PAH degradation assays were conducted in triplicates. Bottles were sealed using rubber stoppers and aluminum crimp seals and shaken at 200 rpm for 24 h at 30 °C. The bacteria were centrifuged to pellet cells (5min, 5k in Sorvall, SL-50T rotor, Sorvall Super T21) and the supernatant was transferred to serum bottles. Three extractions of 0.5 volumes of ethyl acetate (Kodak, Rochester, NY) were performed to extract NP from the aqueous phase. Following extraction, the organic layers were combined and dried with approximately 4 g of anhydrous sodium sulfate (SIGMA, St. Louis, MO). The “dry” liquids were filtered using a 50 mL Erlenmeyer filter flask and a Hirsch funnel before transferred to a 100 mL round

bottom flask (RBF) and rotary evaporated (Heidolph**)** to ~1mL volume. Acetone: hexane (1:1) solvent was added to a final volume of 4 mL. The internal standard, butylbenzene (ALDRICH), was added (10 ppm) before 1 µl of the solution was injected into GCMS-QP5000 (Shimadzu) using an RTX-5 column. The GCMS program consisted of 2 min at 40.0 ℃ followed by a 15°C min^{-1} increase to 190 °C and held for 4 min (injection temp 250 ℃, interface temp 280 ℃, and column flow 1.1 mL/min). Hydrogen was used as the carrier gas, "split" control mode was used, and the selective ion monitoring (SIM) mode was utilized to detect low concentrations of naphthalene (Ch1-m/z = 128.2 and Ch2-m/z = 134.2). The concentration of NP was calculated by comparison against NP standard calibration curve (**Figure 8**). Isolate (s) within each group that ranked the highest on the growth, $E_{24,}$ and BATH assays were selected (**Table 8**). Endpoint analyses (measured % NP degradation after 24 hours of incubation) was conducted on isolates NP 504, NP 505, NP 514, NP 520, NP 516, NP 527, and NP 530 (**Figure 9**).

3.6 Bacterial Adhesion to Hydrocarbons (BATH)

Single colonies were aseptically transferred from MSA-N-I into 5 mL MSB containing 50 µl TSB and incubated for 24 hours at RT and 200 rpm. The next day 100 µl was transferred to fresh media and grown for 24 hours at RT and 200 rpm. On the third day bacteria were spun down (5 min at 5800 rpm, SA-600 rotor) washed twice and resuspended in 1.2 mL PUM buffer (2.22 g $K_2HPO_{4,}$ 7.26 g $KH_2PO_{4,}$ 1.8 g urea, 0.2 g $MgSO_4 \cdot 7H_2O$ dissolved in 1000 mL DI water, pH 7.1). The solution was transferred to 10 mm diameter test tubes. The test tubes were diluted as needed by adding PUB buffer until all test tubes had an OD of approximately 0.600. The equipment was blanked with

the PUM buffer. The OD was measured and recorded by pipetting 1 mL of solution from each flask into a cuvette. The cuvettes were placed in a Vernier spectrophotometer and analyzed by a Vernier Spectral Analysis software (Vernier). Absorbances were recorded at 400 nm. Next, 0.2 mL of hexadecane was added to each test tube. After preincubation (25 °C for 10 min), the mixtures were agitated for 2 min. Following agitation, the solutions were left at room temperature for 15 min to allow separation of aqueous and organic layer. The OD of the aqueous phase was again measured and recorded. Assays were carried out in triplicates. Adhesion to hydrocarbons was calculated as follows: $H=[1-A/A_0] *100$. A_0 is the absorbance of the bacterial suspension without the hydrophobic phase. A is the absorbance after mixing with hexadecane (Charan 2017).

3.7 Emulsification Activity Assay [E_{24}test]

All ten cultures were inoculated in 5 mL MSB containing 100 ppm naphthalene (25mg mL^{-1} in 95% ethanol) and 10 µl Tryptic Soy Broth (TSB). Cultures were grown for 24 hours at room temperature and 200 rpm. The next day 100 µl was transferred to fresh MSB and grown for 24 hours at room temperature and 200 rpm. *Escherichia coli* and 30 µl Tween®20 were used as negative and positive controls, respectively. Cultures were centrifuged *(*Sorvall® RC 28S) with an SA-600 rotor at 5800 rpm for 5 minutes. The supernatant (4 mL) was pipetted into 20 mL test tubes containing 6 mL hexadecane. The mixtures were homogenized by vortexing at high speed for 2 minutes. After 24 hours, the height of the stable emulsion layer was measured (**Figure 10**). E_{24} index was calculated by divide the height of the emulsification layer by the total height, multiplied by 100 (Cooper and Goldenberg 1987).

3.8 Genome Sequencing and Analysis

Isolates NP504, NP505, NP509, NP514, NP516, NP520, NP523, NP527, and NP530 were sent out for genome sequencing. Genomic DNA was extracted using MasterPure DNA Purification kit protocol from Lucigen (Biosearch Technologies, Hoddesdon, UK). Libraries were prepared for whole genome sequencing (WGS) using the (dilute) Nextera DNA Library preparation kit (Illumina), with 500 - 600 bp insert sizes, 250 bp paired-end reads and were generated on an Illumina HiSeq 1000 instrument (Hubbard Genome Center, University of New Hampshire).

The genomes were annotated in PATRIC (PMID: 31667520) using the Comprehensive Genome Analysis service. They were assembled using Unicycler (Unicycler v0.4.8) (Wick *et al*. 2017) and annotated using RASTtk (PMID: 25666585) (Brettin *et al.* 2015). The "similar genome finder" service was used to identify the closest relatives (Ondov *et al.* 2016). A phylogenetic tree was designed containing 54 reference and representative *Acinetobacter* genomes using Markov Cluster algorithm (MCL) in PATRIC 3.6.12. The tree was constructed with 100 genes with five allowed deletions and duplications (Davis *et al.* 2016) (**Fig. 11**). The nwk tree file was edited using Geneious prime 2022.1.1 (https://www.geneious.com).

Biphenyl catabolic genes were identified by investigating proteins annotated to be involved in the biphenyl degradation pathway. PAH catabolic genes were identified using the "protein family sorter" tool in PATRIC 3.6.12. Heatmap function within the "protein family sorter" tool was utilized to identify the number of identical and total proteins in

each isolate (Lindemann *et al*. 2016). Genome browser in PATRIC was utilized to search for potential catabolic operons surrounding the genes of interest (Brettin *et al.* 2015)**.**

BLASTx searches and GC content analysis on target genes and neighboring genes were done to assess homology and potential HGT (Altschul *et al.* 1990) ("Calculator for Genetic Nitrogenous Bases")**.** Similarity between the aromatic RHD α subunit identified in our isolates and naphthalene dioxygenase iron sulfur protein (*nah*Ac) from *Pseudomonas putida* 3IA2NH (Accession: AF306436.1) was assessed by Global Align (Altschul *et al*. 1990). Average nucleotide identity (ANI) analysis was performed with the ANI calculator (http://enve-omics.ce.gatech.edu/ani/) to assess DNA sequence identity between the groups. Finally, the pathogenicity towards human hosts was predicted by Pathogen Finder 1.1 (Cosentino *et al.* 2013).

3.9 Reverse Transcription PCR

Nucleotide sequences of target genes were transferred from PATRIC 3.6.12 (Wattam *et al.* 2014) to Geneious prime 2022.1.1 (https://www.geneious.com) where primer sequences were manually selected. Sequences, about 300 nucleotides apart, of ~18 nucleotides were selected from the center of the gene. The melting points were ~ 53 °C. The primer combinations in **Table 1** were used to amplify the aromatic ring hydroxylating dioxygenase alpha subunit (~290 bp). The 16S rRNA gene-specific primers 515F and 926R were used as positive control. Primers were ordered from Eurofins Genomics (Louisville, KY) and suspended in DNA rehydration solution (Promega) to make 100 μM master stocks. Working stocks (10 μM) were made by diluting the master stocks with nuclease-free water (Promega). Colony touch PCR was

performed to test the primers. PCR on extracted gDNA (Monarch Genomic DNA Purification Kit, Rowley, MA) was performed on isolates 504, 520, and 523. Gel electrophoresis, as described earlier, was used to view the results.

Experimental treatments were grown on 5 mL MSM supplemented with 100 ppm NP and control treatments grew on 5 mL MSM supplemented with 500 µl of both TSB (Becton Dickinson, USA) and dextrose (J. T. Baker, Phillipsburg, N.J). Test tubes were incubated at ~ 30 °C and 200 rpm. Tubes were re-transferred twice by transferring 100 µl of growth to fresh media. On the day of RNA extraction, the tubes were transferred again and grown for 7 hours to have fresh actively growing cells. OD was recorded as described earlier to assess growth. Three mL and five mL were used to extract RNA from experimental and control treatments, respectively. Total RNA extractions were performed using the SV Total RNA Isolation kit according to the recommendations of the manufacturer (Promega, Madison, WI), and the extracts were further purified by DNase I treatment according to the instructions of the kit manufacturer (Promega, Madison, WI).

The reverse transcriptase PCRs (RT-PCRs) were performed in 13 µl with ~1 ng μl^{-1} of total RNA with the OneStep RT-PCR kit (Promega, Madison, WI). The thermocycler program used for the RT-PCRs was as follows: 50°C for 20 min, 95°C for 2 min, 45 cycles (95°C for 20 s, 55°C for 30 s, and 72°C for 1 min), and 72°C for 5 min. The results were analyzed on a 2% agarose gel as described previously.

Table 1. Primer sets used during polymerase chain reaction (PCR) and reverse transcription PCR (RT-PCR) for PAH catabolic genes and 16S rRNA. PCR was conducted on *pahE* and 16S rRNA for all isolates bacteria using genomic DNA template (Hong Sunhee 2016; Liang, Huang and Wang 2019). Reverse transcription PCR (RT-PCR) was conducted on aromatic RHD α subunit (Groups A, B, and C) for sequenced isolates using extracted RNA. The last two rows display the primer sets used to amplify biphenyl-2,3-diol 1,2-dioxygenase III (BphC) for sequenced isolates.

Primer Name	Forward and Reverse Primer	Expected Band Size
16S rRNA	27F: AGAGTTTGATCCTGGCTCAG 1492R: TACCTTGTTACGACTT	1500
pahE	1F: TGCGGCGGGTGTNAAYGGNAT 1R: CCTGAGGAATCTCGGACATYTSTGCCCARAA	370
RHD (Group A)	F: CCAGGTAACTGGAAAATCC R: CTAATTCTTCATGACCTTCG	280
RHD (Group B)	F: GGGAACTGGAAAATCCAG R: CTTCTAATTCTTCATGGCC	280
RHD (Group C)	F: CGGGTAACTGGAAAATCC R: CGACTGCACGAACAATAC	300
BphC Group A and Group B	F: CTACCTGTCATTTCTATCAAAC R: CTTCTGAAATGGGAGTGTC	200
BphC 516	F: CTATCAAACCGTATTAGGG R: CCACTTCTGAAATAGGAG	200

CHAPTER IV

RESULTS

4.1 Isolation and Identification of NP Degrading Bacteria

Thirty-two bacteria were isolated from urban soil. They were selected based on their ability to convert indole to indigo, a phenotypical trait of naphthalene dioxygenase activity (Mercadal *et al.* 2010). BLAST analysis revealed that the top blast matches to the 16S rRNA were the same for many of the isolates Blast analysis revealed five groups, the biggest being 25 *Acinetobacter seifertii* strain LUH 1472. Four isolates matched *Acinetobacter pittii* DSM 21653 strain ATCC 19004, one isolate matched *Acinetobacter baumannii* strain DSM 30007, one matched *Rhodococcus agglutinans* strain CFH S0262 and one matched *Salmonella enterica subsp. enterica* strain LT2 (**Table 2**).

The main two groups, *A. seifertii* and *A. pittii*, are both emerging pathogens resistant to many antibiotics (Li *et al.* 2017; Furlan *et al.* 2019). *A. baumannii* is a well-known opportunistic hospital acquired pathogen (Furlan *et al.* 2019). *R. agglutinans* is a Gram-positive, aerobic, non-motile and non-spore forming bacteria (Guo *et al.* 2015). Finally, *S. enterica* is a facultative anaerobic Gram-negative bacterium that are known animal and human pathogens (Andino and Hanning 2015)

PCR analysis revealed that the *R. agglutinans* isolate and eight *A. seifertii* isolates contained the PAH hydratase-aldolase (*pahE)* gene. This is a catabolic gene that

catalyzes the fifth step in PAH degradation pathway by converting trans-o-hydroxybenzylidenepyruvate (tHBPA) to aldehydes and pyruvic acid (Liang, Huang and Wang 2019) (**Table 2**). Ten isolates were chosen for further study based on top BLAST matches and the presence of the *pahE* gene.

4.2 Growth Assays

Growth of the isolates was assessed on NP, BP, and PH with isolates revealing different growth preferences. NP505 grew best on PH reaching an OD of 0.94 (group A) (**Figure 5**). NP504 reached the highest OD (0.71) on BP and NP514 grew best on PH reaching an OD of 0.77 (group B). NP509, NP515, NP520, and NP523 grew best on BP reaching an OD of 0.66, 0.63, 0.65, and 0.70, respectively. Interestingly, growth on BP had a longer lag phase (**Figure 6**). Finally, NP516, NP527, and NP530 grew best on NP reaching an OD of 0.77, 0.70, and 0.78, respectively (group C) (**Figure 4**). The majority (5/10) of the isolates reached the highest OD with BP as the growth substrate. Isolates in group A and B appear to grow better on the PH while isolates in group C appear to grow better on NP and BP.

Control growth assays were performed to confirm that the isolates were utilizing the PAHs as the main carbon and energy source. The first control growth assay was done with naphthalene dissolved in ethanol and no additional TSB (**Figure 7**). The optical densities after 24 hours were compared using a paired two-tailed t-test and revealed that the growth was significantly different (**Table 4**). Cultures grown without TSB reached a higher OD in 8/10 isolates. Small differences such as the temperature in the laboratory may have affected the growth.

A second control growth assay was done with TSB as the only available carbon source. The bacteria grew poorly indicating that the addition of TSB to the growth assays did not support the growth observed in PAH growth assays. Adding the results from the second control growth assay to the growth assays on NP, PH, BH, containing TSB, did not significantly change the results (**Table 4**). The third and final growth assay was done with the solvent, ethanol, as the sole carbon and energy source. The growth assay revealed that the bacteria were able to survive and grow with ethanol being the only available carbon source. Statistical analysis revealed that the results from growth assays containing NP dissolved in ethanol (without TSB) were significantly different from the growth assays containing only ethanol. All isolates except NP520 grew better on NP + ethanol than on ethanol alone. Therefore, the results indicate that the bacteria can metabolize naphthalene as they reach a higher OD when NP is present in the media.

4.3 PAH Quantification

Naphthalene degraders degraded 83.2- 92.9 % of NP in 24 hours. Control flasks lost 22.46 % of NP after incubation and extractions and so the results are corrected for this abiotic loss. Group A degraded 92.1 %, group B degraded an average of 83.6 %, and group C degraded an average of 89.0 % of NP (**Table 5**) (**Figure 9**).

4.4 BATH Test

The BATH test measures the degree of adherence of bacterial cells to liquid hydrocarbons. Adherence to hexadecane was determined by assessing the decrease in OD of the aqueous phase after mixing. *Escherichia coli* is known to not adhere to liquid

hydrocarbons and was used as the negative control. The solutions were visibly more transparent after mixing with hexadecane. The number of bacteria cells in the aqueous phase decreased in all assessed with isolate NP509 decreasing the most with a mean of 96.7 ± 2.1 %. NP516 decreased the least with an adhesion of 85.2 ± 2.9 %. The negative control decreased by 2.6 ±1.7 % after mixing. The values are the average of three replicates for each isolate. The results indicate that the bacteria can adhere to liquid hexadecane and likely other hydrophobic compounds such as PAHs (**Table 7**).

4.5 Emulsification Activity (E_{24})

The emulsification activity assay screens for biosurfactant producing bacteria. The emulsification activity assay revealed that isolate NP505 was the best emulsifier with a mean of 55 %. The result indicates that NP505 produce a lot of biosurfactants as it could emulsify high into the hydrophobic layer. The 2nd and 3rd best emulsifiers were isolates NP530 (16 %) and NP516 (12 %), respectively (**Figure 10**). *Escherichia coli* was the negative control bacterium and Tween 20 (positive control) is a detergent that will emulsify the hexadecane. All the isolates performed better than the negative control.

4.6 Genome Analysis

Assembly and annotation key results can be found in **Table 9**. The isolates have a G+C content of 38.28-38.72. The number of protein coding genes (with functional assignment) ranges from 2488-2560. The number of protein coding genes (without functional assignment) range from 1102-1207. The number of coding sequences (CDS) range from 3662-3712. Similar genome finder tool (all public genomes) in PATRIC

(PMID: 31667520) revealed that all the isolates belong to the genus *Acinetobacter* and that they can be arranged into three groups (A, B, C) (Ondov *et al.* 2016). The top match for isolate 505 was *A. pittii* strain Aci00905 (group A) (k-mer count 496/1000) (GenBank accession CAJHHN000000000). *A. pittii* strain Aci00905 was isolated from a human host in Germany, 2018. This study focused on human pathogens and strategies to reduce the risk of epidemics (Ondov *et al.* 2016). The top match for isolates 504 and 514 was *A. pittii* strain KCJK1729 (group B) (k-mer count average 391.5/1000) (GenBank accession LYQN00000000.1). *A. pittii* strain KCJK1729 was isolated from the feces of beef cattle (Bos taurus) in the USA, 2015. This study found naturally occurring cefotaxime resistance microbes in beef cattle (Ondov *et al.* 2016). Finally, the top match for isolates 509, 516, 520, 523, 527, and 530 was *A. seifertii* strain SAb133 (group C) (k-mer count 434/1000) (GenBank accession SNSA00000000). *A. seifertii* strain SAb133 was isolated from soil samples in Brazil, 2015. This study found that the strain carried heavy metal resistant genes (Ondov *et al.* 2016). None of the top genome matches were reported to degrade PAHs.

Average nucleotide identity (one-way ANI2) analysis was performed on one isolate from each group to assess similarity among the groups. Isolate 504 was selected to represent group B and isolate 509 was selected to represent group C. The DNA sequence identity between group A and group B is 96.09% (SD: 3.09%), the identity between group A and C is 87.24% (SD: 5.12%), and the identity between group B and group C is 87.30% (SD: 5.15%).

Phylogenetic analysis of the isolate genomes and a collection of reference *Acinetobacter* genomes revealed that all three groups are located in the same cluster

indicating that the groups are closely related, as previously indicated by ANI analysis (**Figure 11**).

Potential PAH catabolic genes were identified by investigating proteins assigned to benzoate, biphenyl, and naphthalene pathways in PATRIC 3.6.12 and by searching for common PAH catabolic genes using the "protein family sorter" tool (Lindemann *et al*. 2016). Despite being successfully amplified in six of the sequenced *Acinetobacter* isolates, the *pahE* gene was not identified during genome analysis. Sequencing of these amplicons should be done to identify PCR product. The "protein family sorter" tool revealed homologs to benzoate 1,2-dioxygenase α subunit (EC 1.14.12.10) in all isolates. Biphenyl-2,3-diol 1,2-dioxygenase III (EC 1.13.11.39) was identified in isolates NP504, NP505, NP514, and NP516. Benzoate 1,2-dioxygenase α subunit and biphenyl-2,3-diol 1,2-dioxygenase III were annotated to be involved in the benzoate degradation pathways via hydroxylation and biphenyl degradation, respectively. According to the Kyoto Encyclopedia of Genes and Genomes (KEGG) benzoate 1,2-dioxygenase α subunit (EC 1.14.12.10) is an oxidoreductase that acts on paired donors with incorporation or reduction of molecular oxygen. Biphenyl-2,3-diol 1,2-dioxygenase III, often called BphC, is involved in the degradation of biphenyl and catalyzes the meta-cleavage reaction by incorporating two oxygen atoms (Kanehisa *et al.* 2016).

Benzoate 1,2-dioxygenase α subunit was selected as our target gene as BLASTx analysis revealed that the nucleotide sequences from the majority of the isolates closely matched the aromatic RHD α subunit from *Acinetobacter* isolates in the GenBank database (**Table 11**). The benzoate 1,2-dioxygenase α subunit gene from groups A, B, and C, excluding NP514 and NP530, matched the aromatic RHD α subunit genes with

99.1-100 % identity (Altschul *et al.* 1990; Brettin *et al.* 2015). The aromatic RHD α subunit from NP505 (group A) is 40 % identical to naphthalene dioxygenase iron sulfur protein (*nahAc*) from *Pseudomonas putida* 3IA2NH (Accession: AF306436.1). The aromatic RHD α subunit from NP504 (group B) and NP 509 (group C) are 43 % identical to naphthalene dioxygenase iron sulfur protein (*nahAc*) from *P. putida* 3IA2NH (Accession: AF306436.1) (Altschul *et al*. 1990). The biphenyl-2,3-diol 1,2-dioxygenase III gene from NP504, NP505, NP514, and NP516 matched VOC family protein with 97.7-100 % identity (Li *et al.* 2009) (**Table 11**).

The PATRIC Heatmap tool revealed that all isolates contained one copy of the aromatic RHD α subunit gene and that groups A and B plus isolate NP516 contained the biphenyl-2,3-diol 1,2-dioxygenase III gene. In addition, all isolates contained the aromatic RHD β subunit. The GC content of the biphenyl-2,3-diol 1,2-dioxygenase III gene ranged from 36.7-37.7 while the GC content of the aromatic RHD α subunit gene ranged from 42.8-43.6 %. Finally, BLASTx analysis of genes surrounding the target genes suggested that no HGT had taken place as top blast matches were all to *Acinetobacter* genes.

4.7 Reverse Transcription PCR

The aromatic RHD α subunit gene was successfully amplified in all isolates confirming its presence in the genomes and that the primers were correctly designed (**Figure 12**). The biphenyl-2,3-diol 1,2-dioxygenase III gene was successfully amplified in NP505 and NP516. The results from isolate NP504 and NP514 are ambiguous and should be repeated (**Figure 12**). Aromatic RHD α subunit was expressed by isolates

NP509, NP520, and NP530 during growth on both experimental (PAH) and control (TSB and dextrose) treatments which suggests it is constitutively expressed in those isolates. In contrast, the aromatic RHD α subunit was only expressed in isolates NP504, NP514, NP516, NP523, and NP527 when grown in the control treatments. However, the results are inconclusive as our positive control 16S rRNA was only amplified in the control treatments of isolates NP504, NP505, NP514, NP527, and NP530 (**Figure 13**). The 16S rRNA gene is a housekeeping gene and should be constitutively expressed during growth in both treatments (Volokhov *et al.* 2007).

Table 2. Top 16S rRNA BLAST matches from the GenBank database and the presence of *pahE* gene.

Isolate	Top Blastn match:	Accession Number:	Percent Identity:	*pahE* PCR
NP 501	*Acinetobacter seifertii* strain LUH 1472	NR_134684.1	99.88	-
NP 502	*Acinetobacter seifertii* strain LUH 1472	NR_134684.1	98.87	-
NP 503	*Acinetobacter seifertii* strain LUH 1472	NR_134684.1	99.88	-
NP 506	*Acinetobacter seifertii* strain LUH 1472	NR_134684.1	99.88	-
NP 507	*Acinetobacter seifertii* strain LUH 1472	NR_134684.1	99.21	-
NP 508	*Acinetobacter seifertii* strain LUH 1472	NR_134684.1	99.29	-
NP 511	*Acinetobacter seifertii* strain LUH 1472	NR_134684.1	99.21	-
NP 512	*Acinetobacter seifertii* strain LUH 1472	NR_134684.1	99.18	-
NP 513	*Acinetobacter seifertii* strain LUH 1472	NR_134684.1	99.18	-
NP 515	*Acinetobacter seifertii* strain LUH 1472	NR_134684.1	99.57	+
NP 516	*Acinetobacter seifertii* strain LUH 1472	NR_134684.1	99.65	+
NP 519	*Acinetobacter seifertii* strain LUH 1472	NR_134684.1	99.88	-
NP 520	*Acinetobacter seifertii* strain LUH 1472	NR_134684.1	99.88	+
NP 521	*Acinetobacter seifertii* strain LUH 1472	NR_134684.1	99.17	-
NP 522	*Acinetobacter seifertii* strain LUH 1472	NR_134684.1	99.88	+
NP 524	*Acinetobacter seifertii* strain LUH 1472	NR_134684.1	99.21	+
NP 525	*Acinetobacter seifertii* strain LUH 1472	NR_134684.1	99.53	ND
NP 526	*Acinetobacter seifertii* strain LUH 1472	NR_134684.1	99.88	ND

Table 2, Cont.

Isolate	Top Blastn match:	Accession Number:	Percent Identity:	*pahE* PCR
NP 527	*Acinetobacter seifertii* strain LUH 1472	NR_134684.1	99.3	+
NP 528	*Acinetobacter seifertii* strain LUH 1472	NR_134684.1	98.65	+
NP 529	*Acinetobacter seifertii* strain LUH 1472	NR_134684.1	93.83	-
NP 530	*Acinetobacter seifertii* strain LUH 1472	NR_134684.1	99.88	+
NP 531	*Acinetobacter seifertii* strain LUH 1472	NR_134684.1	99.41	-
NP 532	*Acinetobacter seifertii* strain LUH 1472	NR_134684.1	99.21	-
NP 504	*Acinetobacter pittii* DSM 21653 strain ATCC 19004	NR_117621.1	99.65	-
NP 505	*Acinetobacter pittii* DSM 21653 strain ATCC 19004	NR_117621.1	99.77	-
NP 514	*Acinetobacter pittii* DSM 21653 strain ATCC 19004	NR_117621.1	99.79	-
NP 518	*Acinetobacter pittii* DSM 21653 strain ATCC 19004	NR_117621.1	98.82	-
NP 509	*Acinetobacter baumannii* strain DSM 30007	NR_117677.1	97.44	-
NP 510	*Salmonella enterica* subsp. enterica strain LT2	NR_104709.1	99.53	-
NP 523	*Rhodococcus agglutinans* strain CFH S0262	NR_136860.1	100	+

Table 3. Growth assay comparisons based on different growth media. All numbers represent the OD 600 after 24 hours.

Groups	Isolate	PH + TSB	BP + TSB	NP + TSB	NP (In Ethanol)	95% EtOH	TSB
A	505	0.94	0.63	0.62	1.02	0.81	0.008
B	504	0.54	0.71	0.62	0.70	0.58	0
	514	0.77	0.74	0.77	0.58	0.57	0.005
	509	0.64	0.66	0.52	0.80	0.63	0
	515	0.54	0.63	0.61	0.69	0.41	0
	516	0.41	0.47	0.77	0.70	0.43	0
C	520	0.35	0.65	0.54	0.95	1.06	0
	523	0.47	0.70	0.56	0.91	0.53	0
	527	0.30	0.62	0.70	0.92	0.64	0.002
	530	0.50	0.25	0.78	1.03	0.95	0.006

Table 4. Statistical comparisons (paired two-tailed t-test) of the OD after 24 hours between different growth assays.

Growth Media Comparison		p-value
NP	95% EtOH	0.0055
NP	NP + TSB	0.0193
PAH + TSB	Addition of Only TSB	0.0589

Table 5. Percent degradation of NP after 24 hours of incubation. NP was quantified using GC-MS and data in this figure are corrected for abiotic NP loss. Values are presented as the average of three independent measurements with respective standard error.

Groups	Isolate	% NP Degradation	Standard Error (SE)
A	505	92.1	1.5
B	504	83.2	3.4
	514	83.9	1.8
C	516	88.5	1.8
	520	90.7	1.2
	527	84.0	2.0
	530	92.9	1.6

Table 6. Comparison between growth on NP versus degradation of NP (%). The results are presented in chronological order with isolates reaching the highest OD on the first control growth assay and the isolates degrading the most NP at the top of the columns. Exception: NP516 removed more NP than NP527 (*).

	Growth on NP *vs.* Degradation of NP	
Isolate	**OD_{600}**	**% Degradation**
530	1.03	92.93
505	1.02	92.07
520	0.95	90.65
527*	0.92	84.03
516*	0.70	88.48
504	0.70	83.94
514	0.58	83.20

Table 7. Results of BATH Test. Adherence capacity of cells to hexadecane in percentage with *Escherichia coli* as the negative control. Values are presented as the average of three independent measurements with respective standard error.

Isolate No.	Hexadecane Adherence
504	86.9 ±2.491%
505	92.1 ±1.245%
509	96.7 ±2.135%
514	89.3 ±6.527%
515	96 ±2.182%
516	85.2 ±2.902%
520	96.3 ±1.905%
523	90.5 ±2.281%
527	91.6 ±4.283%
530	89.8 ±3.348%
Escherichia coli	2.6 ±1.72%

Table 8. Growth, E_{24} and BATH assays ranking of selected isolates.

Isolate	Genus & species	Growth rank NP	Growth rank PH	Growth rank BP	E_{24} rank	BATH Assay	*pahE* +/-
505	*A. pittii*	6	1	7	1	4	-
530	*A. seifertii*	1	6	10	2	7	+
514	*A. pittii*	3	2	1	9	8	-
527	*A. seifertii*	4	10	8	3	5	+
516	*A. seifertii*	2	8	9	4	10	+
523	*R. agglutinans*	8	7	3	6	6	+
520	*A. seifertii*	9	9	5	8	2	+
515	*A. seifertii*	7	4	6	7	3	+
509	*A. baumannii*	10	3	4	10	1	-
504	*A. pittii*	5	5	2	5	9	-

Table 9. Key assembly and annotation results of the sequenced *Acinetobacter* isolates.

Isolate	Average Short Read Coverage	Total Contigs	GC Content	Genome Length (bp)	Protein encoding genes with functional Assignment	Protein encoding genes without functional Assignment	CDS	rRNA
504	601.379	34	38.71	3885964	2555	1107	3,662	3
505	757.994	34	38.72	3886546	2534	1136	3,670	3
509	425.624	13	38.28	3908436	2489	1200	3,689	4
514	404.126	32	38.71	3885895	2560	1102	3,662	3
516	369.649	13	38.33	3943488	2505	1207	3,712	3
520	454.409	14	38.28	3908852	2490	1202	3,692	3
523	597.4	13	38.28	3908186	2489	1199	3,688	3
527	621.748	13	38.28	3908449	2489	1203	3,692	3
530	749.789	12	38.28	3908178	2488	1203	3,691	3

Table 10. Closest relatives of sequenced isolates according to "similar genome finder" tool on PATRIC 3.6.12. (All public genomes) (Wattam *et al*. 2014; Ondov *et al*. 2016).

Groups	Isolate	Closest Relative	K-mer Count
A	**505**	*Acinetobacter pittii* strain Aci00905	496/1000
B	**504**	*Acinetobacter pittii* strain KCJK1729	392/1000
	514	*Acinetobacter pittii* strain KCJK1729	391/1000
C	**509**	*Acinetobacter seifertii* strain SAb133	434/1000
	516	*Acinetobacter seifertii* strain SAb133	434/1000
	520	*Acinetobacter seifertii* strain SAb133	434/1000
	523	*Acinetobacter seifertii* strain SAb133	434/1000
	527	*Acinetobacter seifertii* strain SAb133	434/1000
	530	*Acinetobacter seifertii* strain SAb133	434/1000

Table 11. Blast analysis and GC content of putative PAH degradation genes identified.

Gene	Top Protein Match	Top Match Organism	Accession Number	% Identity	GC Content
Biphenyl-2,3-diol 1,2-dioxygenase III	VOC family protein	*Acinetobacter pittii*	WP_206216930.1	98.4	37
Biphenyl-2,3-diol 1,2-dioxygenase III	VOC family protein	*Acinetobacter calcoaceticus/baumannii* complex	WP_014208236.1	100	37.7
Biphenyl-2,3-diol 1,2-dioxygenase III	VOC family protein	*Acinetobacter calcoaceticus/baumannii*	WP_014208236.1	100	37.7
Biphenyl-2,3-diol 1,2-dioxygenase III	TPA: VOC family	*Acinetobacter nosocomialis*	HCA5284025.1	97.7	36.7

Table 11, Cont.

Isolate	Gene	Top Protein Match	Top Match Organism	Accession Number	% Identity	GC Content
505	benzoate 1,2-dioxygenase α subunit	Aromatic RHD α subunit	*Acinetobacter lactucae*	*WP_016145463.1*	99.8	43
504	benzoate 1,2-dioxygenase α subunit	Aromatic RHD α subunit	*Acinetobacter calcoaceticus/baumannii* complex	WP_005040193.1	99.3	43.6
514	benzoate 1,2-dioxygenase α subunit	Rieske [2Fe-2S] domain	*Acinetobacter calcoaceticus* RUH2202	EEY78326.1	99.1	43.6
509	benzoate 1,2-dioxygenase α subunit	Aromatic RHD α	*Acinetobacter oleivorans*	WP_174765838.1	100	43
516	benzoate 1,2-dioxygenase α subunit	Aromatic RHD α	*Acinetobacter*	WP_224970926.1	99.8	43.1
520	benzoate 1,2-dioxygenase α subunit	Aromatic RHD α	*Acinetobacter seifertii*	WP_200001728.1	100	43
523	benzoate 1,2-dioxygenase α subunit	Aromatic RHD α	*Acinetobacter oleivorans*	WP_174765838.1	100	43.1
527	benzoate 1,2-dioxygenase α subunit	Aromatic RHD α	*Acinetobacter seifertii*	WP_200001728.1	100	43
530	benzoate 1,2-dioxygenase α subunit	Rieske [2Fe-2S] domain protein	*Acinetobacter calcoaceticus* RUH2202	EEY78326.1	99.1	42.8

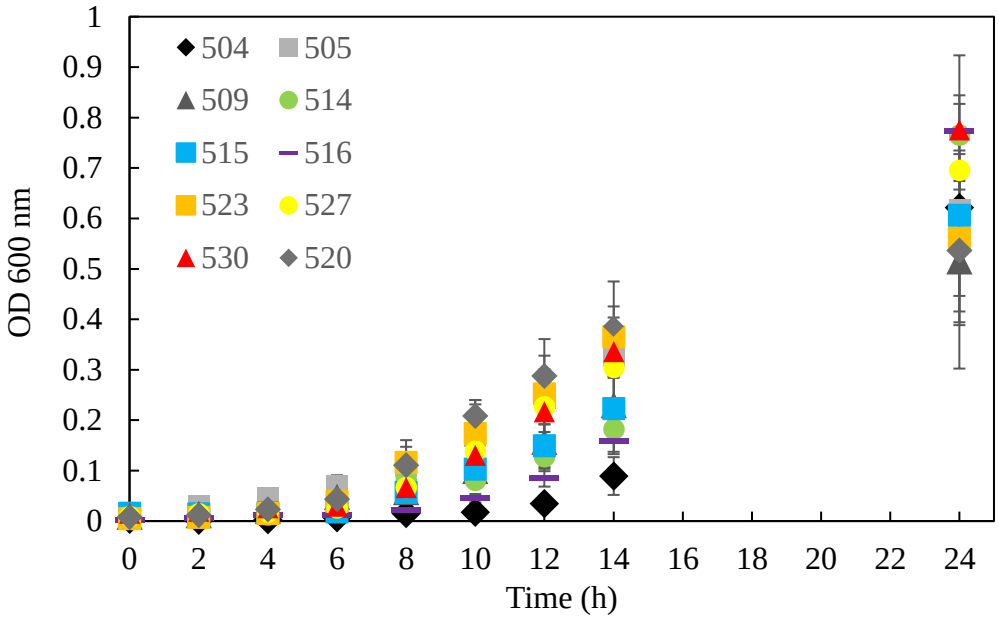

Figure 4. Isolates grown on NP. OD at 600 nm was measured every second hour for 14 hours and again after 24 hours.

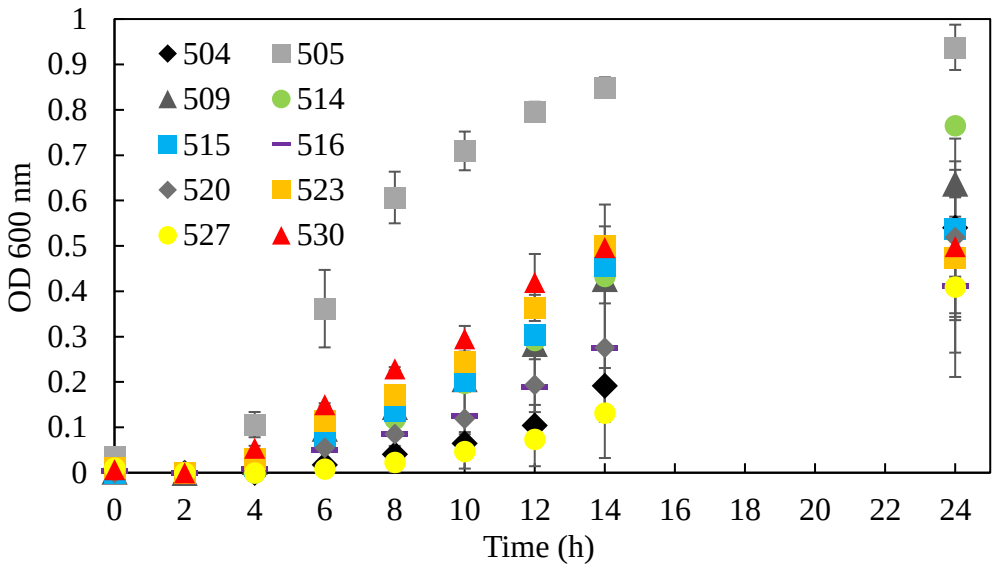

Figure 5. Isolates grown on PH. OD at 600 nm was measured every second hour for 14 hours and again after 24 hours.

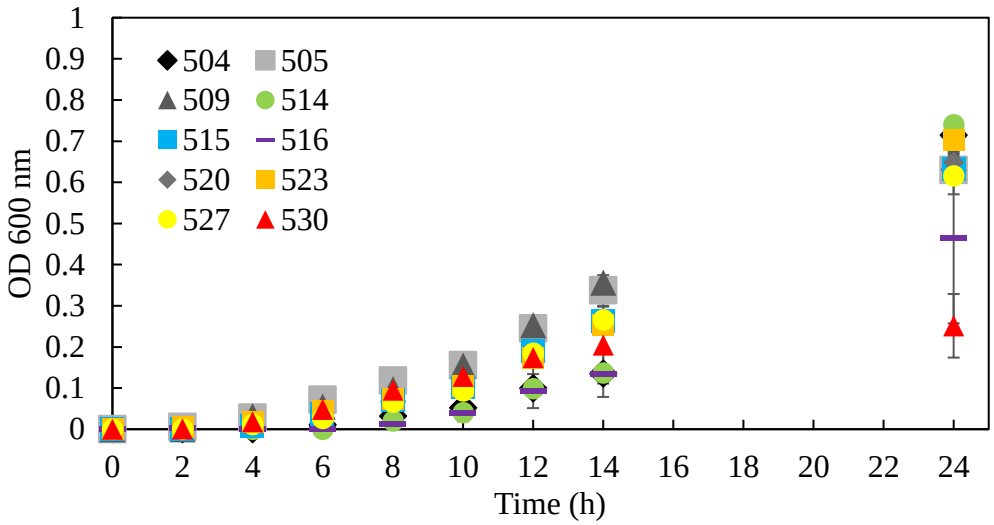

Figure 6. Isolates grown on BP. OD at 600 nm was measured every second hour for 14 hours and again after 24 hours.

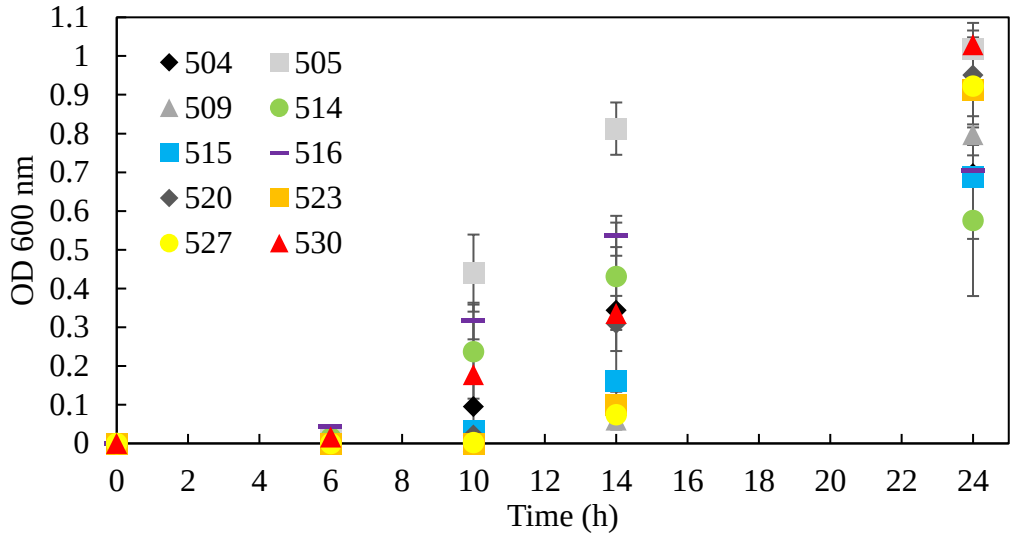

Figure 7. Results from the first control growth experiment. Isolates were grown on 95 % ethanol and the OD was recorded at 600 nm after 6, 10, 14, and 24 hours.

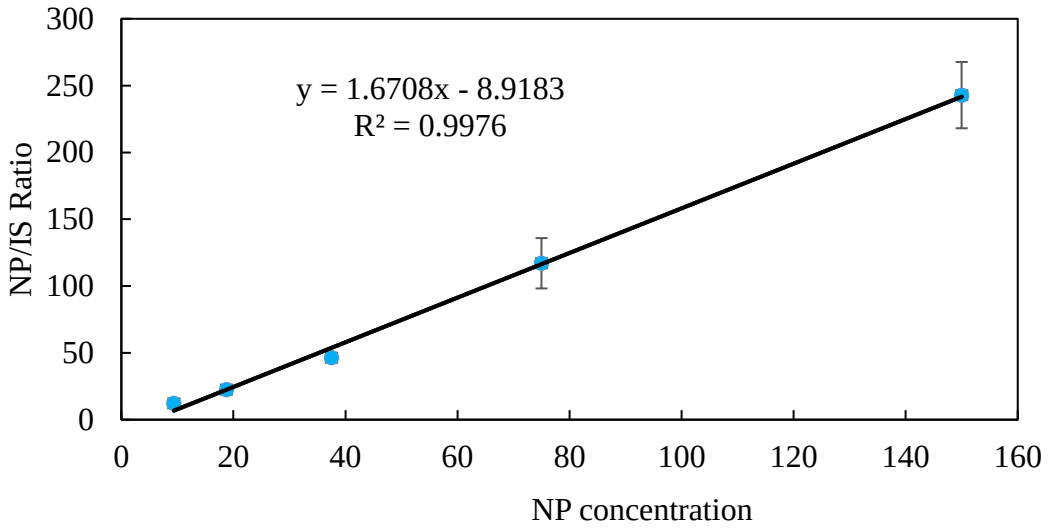

Figure 8. Calibration curve of NP dissolved in acetone:hexane (1:1). A two-fold serial dilution, starting at 150 ppm, was performed. Each datapoint represents the average of three independent replicates with respective standard error bars.

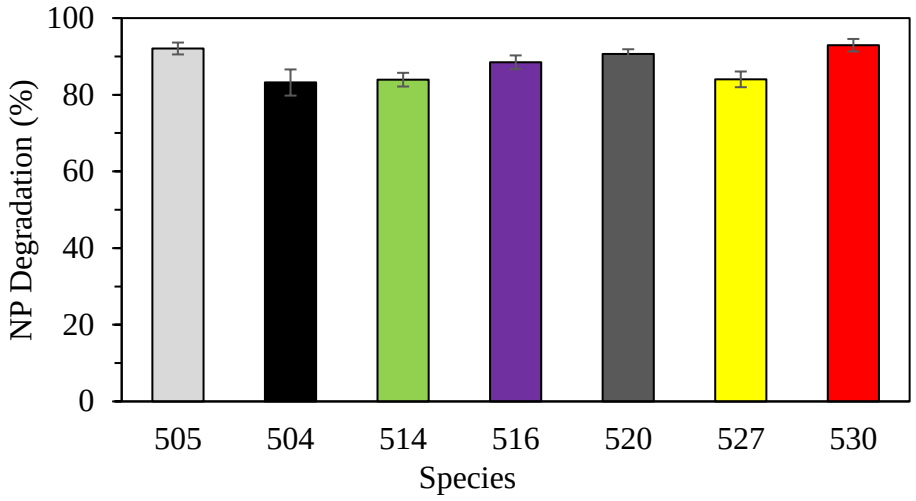

Figure 9. NP degradation by *Acinetobacter* isolates. The isolates were grown with 100 ppm NP. PAH concentration was quantified using GC-MS. The data in this figure are corrected for abiotic NP loss. Values are presented as the average of three independent measurements with respective standard error bars.

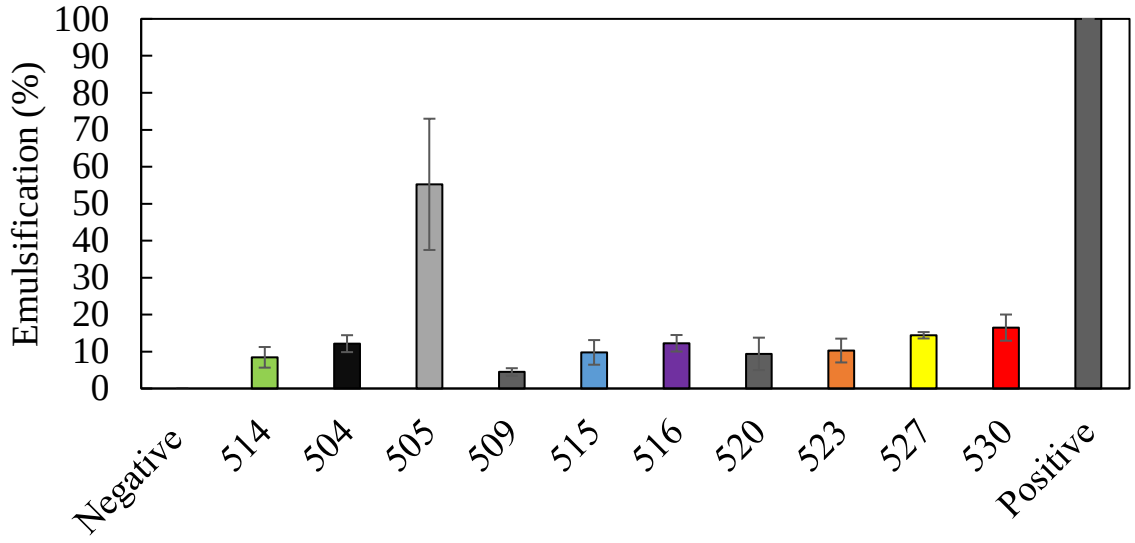

Figure 10. Emulsification activity assay (E_{24}) of selected isolates. Positive control (rightmost column) is Tween 20 and negative control (leftmost columns) is *Escherichia coli*. Values are presented as the average of three independent measurements with respective standard error bars.

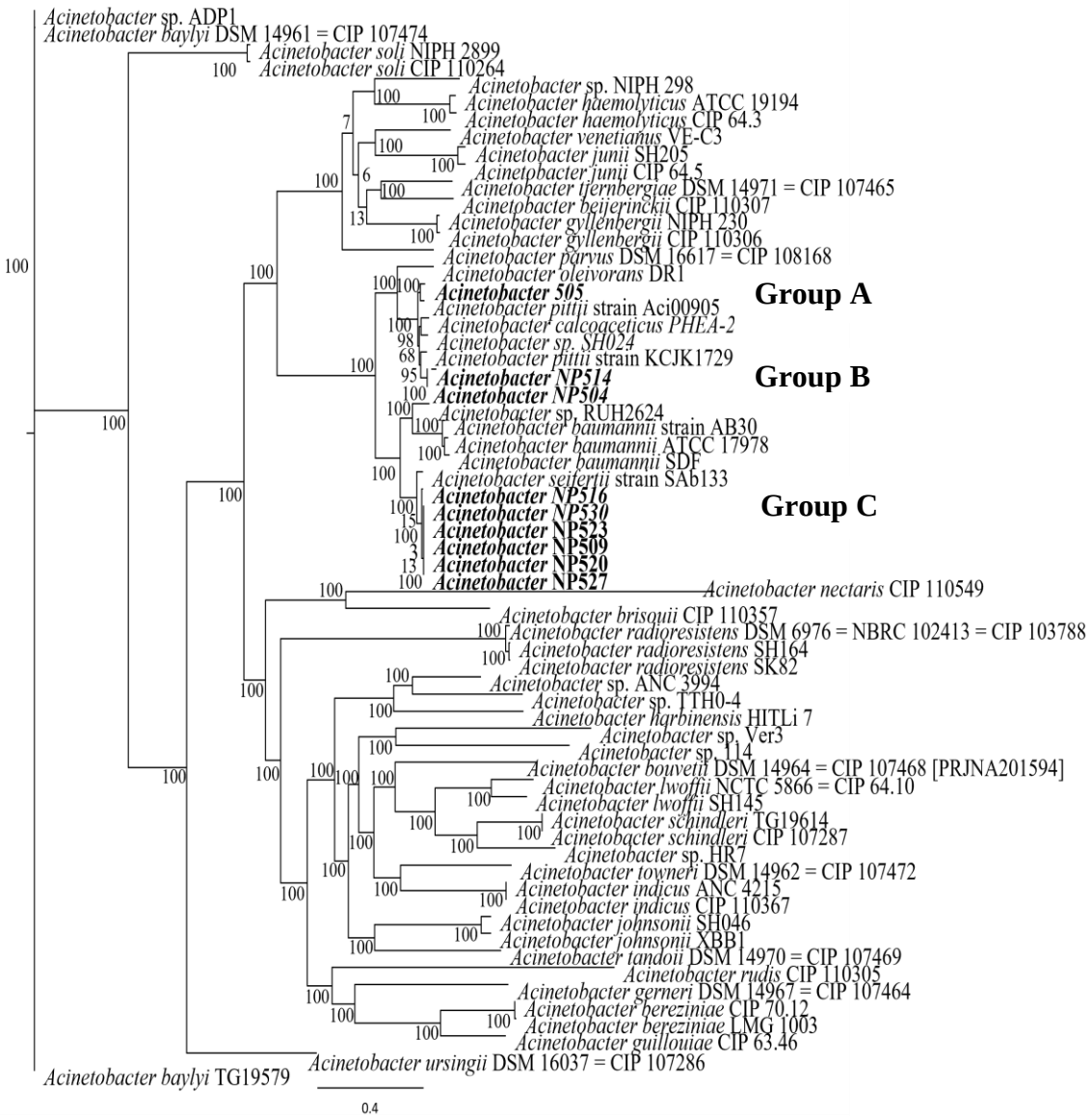

Figure 11. Phylogenetic tree was created, containing 54 reference and representative *Acinetobacter* genomes in PATRIC 3.6.12 (Wattam *et al.* 2014). The parameters were set to 100 genes and five maximum allowed deletions and duplications. The nwk tree file was uploaded to Geneious prime 2022.1.1 (https://www.geneious.com) for editing. Bolded text: isolates from this study (**Table 10**) (Ondov *et al.* 2016).

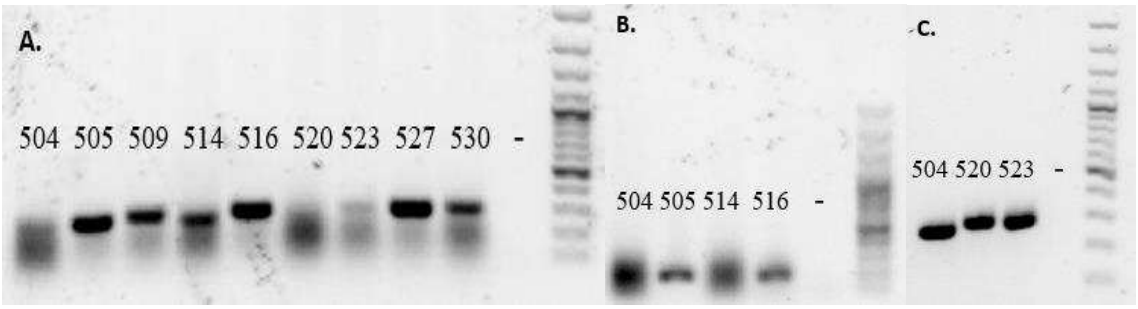

Figure 12. Primer testing of target genes on DNA from sequenced isolates. **A**: aromatic RHD α subunit PCR results. **B**: biphenyl-2,3-diol 1,2-dioxygenase III PCR results. **C**: aromatic RHD α subunit PCR repeat with gDNA of isolates NP504, NP520, and NP523.

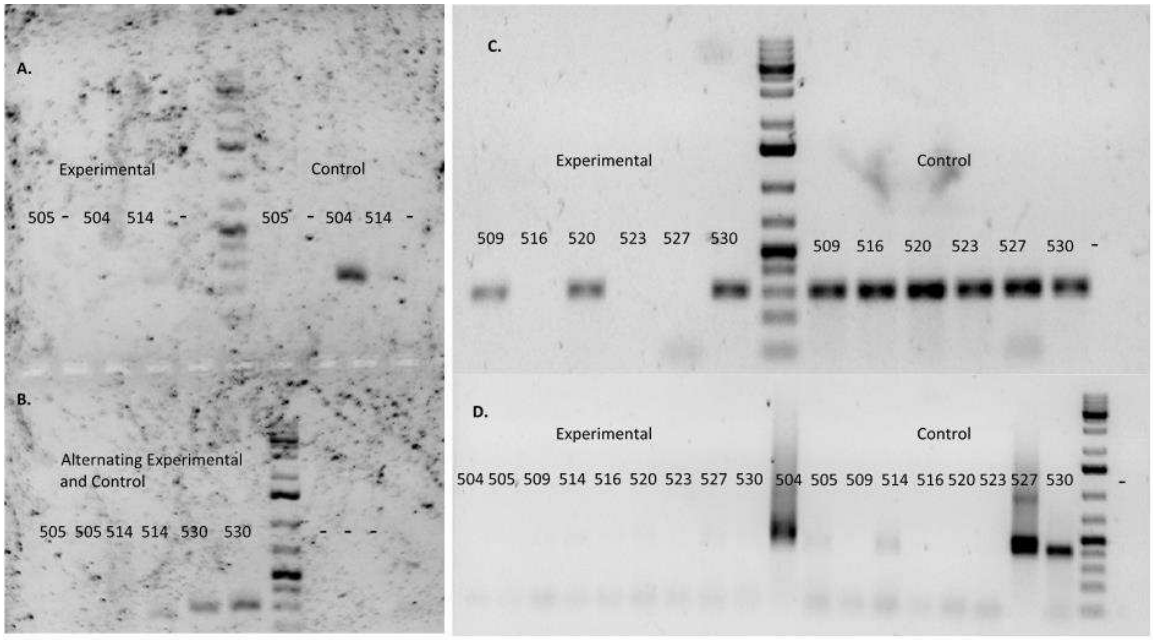

Figure 13. RT-PCR analysis of RHD expression on glucose and NP. **A**: RT-PCR for aromatic RHD α subunit gene (isolates 505, 504, and 514). **B**: RT-PCR results for aromatic RHD α subunit gene (isolates 505, 514, and 530).

CHAPTER V

DISCUSSION

Polycyclic aromatic hydrocarbons are ubiquitous in nature as a result of both natural production and release from anthropogenic activities (Guo *et al.* 2011). PAHs are considered a health hazard due to their well-documented acute toxicity and genotoxicity effects (Takeshita and Kanaly 2019). The negative impacts of PAHs have motivated extensive research to better understand their sources, distribution, toxicity, and environmental fate (Kanaly and Harayama 2010). Various methods have been found to remove PAHs, but bioremediation by bacteria is one of the most prevalent remediation strategies. It is an inexpensive strategy that utilizes microorganisms already present in nature to metabolize and remove PAHs *in situ* (Mohan *et al.* 2006). The most common PAH degrading genera are *Pseudomonas, Sphingomonas, Brevibacterium, Arthrobacter, Nocardioides,* and *Mycobacterium* (Lu *et al.* 2019). *Acinetobacter* is not as well-known as a PAH degrader (Ghosal *et al.* 2013; Shao *et al.* 2015; Jiang *et al*. 2018; Gupta *et al.* 2020).

The goal of this study was to isolate and characterize bacteria able to metabolize PAHs and identify PAH catabolic genes using NP as a model compound. Thirty-two isolates displaying naphthalene dioxygenase activity via conversion of indole to indigo were isolated. Sequencing of the 16S rRNA gene revealed that the majority of the isolates

were members of the genus *Acinetobacter* (**Table 2**). This was surprising as *Acinetobacte*r bacteria are better known as opportunistic human pathogens and relatively few studies have documented PAH bioremediation potential by this genus (Bian *et al.* 2021). PCR detected the *pahE* gene in nine out of the 32 isolates further supporting the ability of the isolates to degrade PAHs (Liang *et al*. 2019). Based on their identity and presence of the naphthalene catabolic gene *pahE,* ten isolates were selected for further study.

Ten isolates were sent out for genome sequencing to analyze their genomes with isolate NP515 omitted due to failure to grow after shipping. All sequenced isolates are members of the *Acinetobacter* genus. Initial 16S rRNA sequencing suggested that NP523 belonged to the *Rhodococcus* genus. However, genome sequencing revealed that it was an *Acinetobacter* isolate. This discrepancy was likely due to mislabeling of a 16S rRNA sequencing sample. Comparison to all public genomes in PATRIC along with phylogenetic analysis revealed that the isolates fell into three groups matching different strains of *Acinetobacter* (**Table 10**).

The genome metrics in our isolates match the expected values found in other *Acinetobacter* isolates (**Table 9**). Chukamnerd *et al.* (2022) isolated 221 *A. baumannii* strains from Clinical Microbiology Laboratories (CMLs) in lower Southern Thailand. Genome analysis of *de novo* assemblies revealed that the isolates had G+C-contents that varied from 38.68% to 39.10%, which is within the same range as my isolates. The genome length of the *A. baumannii* isolates varied from 3,777,937 bp to 4,319,283 bp, with an average of 3,930,367 bp. Again, the genome lengths of my isolates fall within this range. The number of contigs ranged from 26 to 193, with an average of 68. The

number of contigs in our isolates ranged from 12-34, suggesting better coverage of our isolates (Chukamnerd *et al.* 2022). Zhan *et al.* (2012) also identified similar genome metrics in *Acinetobacter calcoaceticus* PHEA-2 as in our isolates (Zhan *et al*. 2012).

According to Pathogen Finder 1.1, all three isolate groups were predicted to be human pathogens. Group A matched 36 pathogenic families and was given a 0.842 probability of being a human pathogen. Groups B (isolates 504 and 514) matched 23 pathogenic families and were given a 0.845 probability of being human pathogens. Finally, all isolates in group C (Isolates 509, 516, 520, 523, 527, 530) matched 18 pathogenic families and were given a 0.863 probability of being a human pathogen (isolate 516 was given a probability of 0.865).

ANI analysis, pathogenicity analysis, and assembly/annotation data suggests that all the isolates contain a similar genome content. However, three distinct groups can be identified. For example, when designing primers for the aromatic RHD α subunit gene, three unique primer sets, one for each group, had to be designed. The pathogenicity analysis also displayed data that could easily be organized in the same three groups as the isolates in each group have the same probability of being a human pathogen.

Genome analysis did not identify the expected naphthalene degrading genes (*nah, phn, dox, and ndo*-like genes) (Yen and Gunsalus 1982; Grund and Gunsalus 1983). Although the gene annotated by PATRIC as benzoate 1,2-dioxygenase α subunit gene blasted as an aromatic RHD α subunit, it did not specify naphthalene RHD α subunit. Sequence identity to *P. putida* NahAc was 40-43 % for NP504, NP505, NP509, suggesting the gene may encode a naphthalene dioxygenase. Genes of interest may have been lost during the sequencing process. Sequencing instrument gives short DNA reads

and sometimes draft genome sequences end up with gaps as evidenced by the presence of multiple contigs rather than one single circular chromosome. Thus, PAH catabolic genes in our *Acinetobacter* isolates may have been located in such gaps or in regions with low sequencing depth. Although it is unlikely that this would occur for all nine isolates sequenced. Alternately, my *Acinetobacter* species may use a previously uncharacterized pathway to initiate PAH degradation. Transcriptomic analysis, which can identify all genes upregulated during PAH degradation, regardless of whether they have previously been described, is one future strategy to identify the PAH degradation genes in my isolates.

The lack of identifiable PAH catabolic genes was surprising as all the isolates could convert indole to indigo which implied naphthalene dioxygenase activity in our isolates (Mercadal *et al.* 2010). It is possible that our isolates contain enzymes capable of catalyzing this reaction but that are not involved in PAH degradation. However, this does not explain the degradation of NP observed in our isolates. It is also possible that genes may have been misannotated in PATRIC. The aromatic RHD α subunit was located shortly upstream from the aromatic RHD β subunit in all isolates. The aromatic RHD α subunit is expected to be involved in NP degradation. However, the RT-PCR results were inconclusive and so we cannot say for sure whether the aromatic RHD α subunit gene we identified is indeed involved in naphthalene degradation.

Despite the failure to definitively identify PAH degradation genes, we observed strong growth on NP, BP, and PH. Large growth differences were observed when grown on different PAHs. For example, NP530 (from group C) reached an OD of 0.78 when grown on NP while a maximum OD of 0.25 was recorded when grown on BP (**Table 8**).

As described previously, groups A and B appear to favor growth on PH while group C performs better on NP and BP. PH contains three fused benzene rings which are thought to be more challenging to degrade than lighter and smaller structures such as NP and BP. GC-MS was used to quantify the removal of NP and revealed that the isolates that reached the highest OD on NP also removed the most NP, confirming that NP is a valid growth substrate for the *Acinetobacter* isolates in this study (**Table 6**). We can only say with certainty that our bacteria can remove NP as we did not quantify PH and BP degradation. Although we did not confirm the removal, we can assume that BP and PH were degraded as the isolates reached similar ODs as when grown on NP and because the different isolates grew distinctively different on the three PAHs. Lee *et al.* (2018) also conducted PAH degradation experiments using a GC-MS and found that PH was utilized as sole carbon source and that the isolates degraded more than 80 % of added PH (*Planococcus halocryophilus, Vibrio alginolyticus, Bacillus algicola, Planomicrobium alkanoclastiucm, and Isoptericola chiayiensis)*. Pyrene, which is a heavier PAH than phenanthrene, was found to be more challenging to degrade. *Cobetia marina, Planococcus halocryophilus, Rhodococcus soli, and Pseudoalteromonas agarivorans* strains were found to degrade 90-99 % of added pyrene. However, the degradation efficiency by the remaining 15 isolates varied from 20-60 %, with the majority removing approximately 40 % of added pyrene (Lee *et al*. 2018).

My results indicate a preference of growth substrate and potentially the presence of different PAH catabolic genes in groups A, B and C (Peng *et al*. 2008). *Acinetobacter* isolates display great genetic and physiological diversity and degradation efficiencies vary depending on genetic makeup and available growth substrate. Thangaraj *et al*.

(2008) identified eleven strains that displayed the ability to degrade various aromatic compounds. Following ten days of incubation an *Acinetobacter* isolate degraded more than 70% of added dibenzofuran, fluorene, and sodium benzoate, with the aromatic growth substrates being the only available energy source. A second *Acinetobacter* isolate removed more than 70% of added biphenyl, dibenzofuran, dibenzothiophene, fluorene, sodium benzoate and salicylic acid (Thangaraj *et al*. 2008). Therefore, *Acinetobacter* isolates can degrade various aromatic compounds, including PAHs, and will likely assist in the removal of harmful pollutants in the environment. Moving forward, genome analysis and identification of PAH catabolic genes should be emphasized as PAH degradation by *Acinetobacter* isolates have been described but little is known about the enzymes catalyzing the degradation.

All nine *Acinetobacter* isolates displayed the ability to grow on more than one PAH, which is an important trait for bacteria used in bioremediation projects. Liu *et al*. (2021) identified *Pseudomonas brassicacearum* strain MPDS which was found to efficiently remove various PAHs and heterocyclic derivatives. MPDS could completely remove 1000 ppm NP in 84 hours. MPDS could also remove 65.7 % of 100 ppm dibenzofuran and 32.1 % of 100 ppm dibenzothiophene in 96 hours. Finally, 40.3 % of 100 ppm fluorene was metabolized in 72 hours. Of the aromatic compounds used in this study, NP is clearly the preferred growth substrate (Liu *et al.* 2021). The efficient NP degradation by my *Acinetobacter* isolates suggests that similar NP catabolic gene clusters may exist between the two species.

The last growth confirmation experiment revealed that all the selected isolates can survive and grow with 95 % ethanol as the sole carbon and energy source making it

challenging to assess the metabolism of the PAHs. Ethanol was used as the solvent to dissolve naphthalene and make the naphthalene mother stock. Ethanol is less harmful to the environment and humans than gasoline. Therefore, to meet new environmental regulations ethanol is continuously taking up a larger portion of gasoline. For example, in Brazil, ethanol content varies between 18 %- 27.5 % (Kirstine and Galbally 2012; de Bruyn *et al.* 2020). The increased use of ethanol is expected to have an impact on ethanol concentrations in the atmosphere. Cities that use ethanol additives have higher ethanol levels in the atmosphere compared to cities that do not. Increased ethanol levels can potentially affect the oxidizing power of the troposphere. Recent studies have also documented that ethanol inhibits the natural anaerobic biodegradation of BTEX compounds (Lovanh *et al*. 2002). Few papers describe ethanol biodegradation, but de Bruyn *et al.* (2020) described that the maximum ethanol degradation rate concurred with the maximum bacterial counts.

Although the ability to metabolize ethanol can be a beneficial trait, it made it challenging to assess the PAH degradation abilities of our isolates. Since the amount of ethanol is the same in every flask the difference in OD between the isolates and the growth assays should relate to the influence of the different PAHs. This thought process was used to compare the growth performance by each isolate and between the different growth assays. Since the isolates can metabolize ethanol, we cannot say whether or not the isolates can survive on NP as a sole carbon and energy source. Growth on PAHs as the sole carbon and energy source should be further researched by utilizing a solvent that my bacteria cannot metabolize such as methanol.

Characterization of surface properties of the isolates helped us understand their ability to degrade hydrophobic PAHs which are challenging to degrade in nature. The BATH test measured the degree of adherence of bacterial cells to liquid hydrocarbons. Bacteria with adhesion abilities are better equipped to degrade PAHs as they adhere to and can access PAHs. Isolates 509 and 520 possess the most hydrophobic bacterial cell surfaces and achieved the highest degree of adherence to liquid hexadecane. However, all isolates performed well, including NP 505, suggesting that all ten *Acinetobacter* isolates are capable of adhering to hydrocarbons. Zita and Hermansson (2006) conducted the BATH test on six different bacterial isolates. *Acinetobacter calcoaceticus* performed the best leaving only 0.3 ± 0.3 % cells in the aqueous phase after partitioning. The results for *Escherichia coli* K51, *Serratia marcescens, Flavobacterium breve*, and *Pseudomonas putida* were 33 ± 012, 1 ± 0, 4 ± 1, and 27 ± 10, respectively (Zita and Hermansson 2006). Chen *et al.* (2013) found that addition of Tween 20 increased bioavailability of pyrene (Chen *et al.* 2013). Abbasnezhad *et al*. (2008) found that the OD of the aqueous phase (*P. fluorescens* LP6a) decreased by 40.5 ± 7.95 after mixing with n-hexadecane when 10 mM buffer amended with $MgSO_4$ was used to wash and resuspend cells. The OD of the aqueous phase of *A. venetianus* RAG1 after mixing with n-hexadecane decreased by 98.98 ± 1.44 when 250 mM potassium phosphate buffer (pH 7) was utilized, similar to results obtained in our study (Abbasnezhad *et al*. 2008) (**Table 7**).

Bacteria with high emulsification activity reduce the interfacial tension between hydrophobic molecules and water. As described earlier this is thought to increase the bioavailability of PAHs and ultimately enhances PAH degradation. Amodu *et al*. (2014) conducted E_{24} assays on *Bacillus licheniformis* STK 01 (BL), *Bacillus subtilis* STK 02

(BS), and *Pseudomonas aeruginosa* STK 03 (PA). BL had an emulsification index of 50 and 70 % on phenanthrene and anthracene, respectively. BS had an emulsification index of 5 and 10 % on phenanthrene and anthracene, respectively. Finally, PA had an emulsification index of 70 and 50 % on phenanthrene and anthracene, respectively (Amodu *et al*. 2014). Ohadi *et al.* (2017) collected soil samples from oil exploration areas and identified *Acinetobacter junii* B6 as the most promising Iranian light crude oil (ILCO) degrader. *A. junii* displayed 51% emulsification of ILCO which is similar to results obtained from NP505 on hexadecane (Ohadi *et al.* 2017). Isolate NP 505 (groups A) performed 38.8 % better than the second-best emulsifier (NP 530) (**Figure 10**). Notably, isolate NP505 is the only isolate in group A and has a more mucoid colony appearance when grown on MSA-N-I than the other isolates.

This study provides evidence that ten *Acinetobacter* isolates can grow on NP, BP, and PH. All research objectives were achieved except experimentally confirming the function of PAH degradation genes due to inconclusive results. The greatest benefit of my study was the NP quantification. The isolates removed close to 100 ppm of NP in only 24 hours. Despite being predicted to be a human pathogen, genome analysis revealed some PAH catabolic genes. My study also provides evidence for production of biosurfactants by *Acinetobacter* isolates.

CHAPTER VII

FUTURE DIRECTIONS

This study has provided valuable information regarding the bioremediation potential of ten *Acinetobacter* isolates. However, future research is needed to improve and verify some of the results. The draft genomes should be completed by pairing our short read dataset with longer reads, such as PacBio, to close the genomes. This may reveal the presence of PAH catabolic genes in our *Acinetobacter* isolates. The lack of annotated NP catabolic genes indicates a need for transcriptomics studies in order to identify any *nah*-like or other PAH catabolic genes transcribed by my bacteria in the presence of NP. Identification of genes used in degrading NP may produce an opportunity to identify a novel or different pathway used by my bacteria to degrade NP. The role of the aromatic RHD α subunit, benzoate 1,2-dioxygenase α subunit or other target genes in PAH degradation may be confirmed by knockout mutagenesis. Another potential approach to verify gene function is to clone any potential PAH degradation genes into an expression vector and measure activity. Moving forward, degradation of phenanthrene and biphenyl should be quantified and compared with the results from NP. Finally, further research should be done to identify an appropriate solvent not metabolized by *Acinetobacter* and assess NP degradation with NP as the only carbon and energy source.

REFERENCES

Abbasnezhad H, Gray MR, Foght JM. Two different mechanisms for adhesion of Gram-negative bacterium, *Pseudomonas* fluorescens LP6a, to an oil-water interface. *Colloids Surf. B* 2008; **62**:36–41.

Abdel-Shafy HI, Mansour MSM. A review on polycyclic aromatic hydrocarbons: Source, environmental impact, effect on human health and remediation. *Egypt. J. Pet.* 2016; **25**:107–23.

Altschul SF, Gish W, Miller W *et al.* Basic local alignment search tool. *J Mol Biol* 1990; **215**:403–10.

Amodu OS, Ntwampe SK, Ojumu TV. Emulsification of hydrocarbons by biosurfactant: exclusive use of agrowaste. *BioResources* 2014; **9**:3508–25.

Andino A, Hanning I. *Salmonella enterica*: survival, colonization, and virulence differences among serovars. *Sci. World J.* 2015; **2015**, DOI: 10.1155/2015/520179.

Bian X, Liu X, Zhang X *et al.* Epidemiological and genomic characteristics of *Acinetobacter baumannii* from different infection sites using comparative genomics. *BMC Genom.* 2021; **22**, DOI: 10.1186/S12864-021-07842-5.

Boonchan S, Britz ML, Stanley GA. Surfactant-enhanced biodegradation of high molecular weight polycyclic aromatic hydrocarbons by *Stenotrophomonas maltophilia*. *Biotechnol. Bioeng.* 1998; **59**:482–94.

Boonchan S, Britz ML, Stanley GA. Degradation and mineralization of high-molecular-weight polycyclic aromatic hydrocarbons by defined fungal-bacterial cocultures. *Appl. Environ. Microbiol.* 2000; **66**:1007–19.

Bosch R, García-Valdés E, Moore ERB. Genetic characterization and evolutionary implications of a chromosomally encoded naphthalene-degradation upper pathway from *Pseudomonas stutzeri* AN10. *Gene* 1999; **236**:149–57.

Bouchez M, Blanchet D, Vandecasteele JP. Degradation of polycyclic aromatic hydrocarbons by pure strains and by defined strain associations: inhibition phenomena and cometabolism. *Appl. Microbiol. Biotechnol.* 1995; **43**:156–64.

Boyd DR, Sheldrake GN. The dioxygenase-catalysed formation of vicinal cis-diols. *Nat. Prod. Rep.* 1998; **15**:309–24.

Brettin T, Davis JJ, Disz T *et al.* RASTtk: A modular and extensible implementation of the RAST algorithm for building custom annotation pipelines and annotating batches of genomes. *Sci. Rep.* 2015, DOI: 10.1038/srep08365.

de Bruyn WJ, Clark CD, Senstad M *et al.* Biological degradation of ethanol in Southern California coastal seawater. *Mar Chem* 2020; **218**, DOI: 10.1016/J.MARCHEM.2019.103703.

Butler CS, Mason JR. Structure-function analysis of the bacterial aromatic ring-hydroxylating dioxygenases. *Adv. Microb. Physiol.* 1997; **38**:75–84.

"Calculator For Genetic Nitrogenous Bases Guanine (G) Or Cytosine (C)". *Sciencebuddies.Org*, 2022, https://www.sciencebuddies.org/science-fair-projects/references/genomics-g-c-content-calculator.

Casillas RP, Crow SA, Heinze TM *et al.* Initial oxidative and subsequent conjugative metabolites produced during the metabolism of phenanthrene by fungi. *J. Ind. Microbiol. 1996 16:4* 1996; **16**:205–15.

Cerniglia CE. Biodegradation of polycyclic aromatic hydrocarbons. *Biodegradation 1992 3:2* 1992; **3**:351–68.

Cerniglia CE, Freeman JP, Mitchum RK. Glucuronide and sulfate conjugation in the fungal metabolism of aromatic hydrocarbons. *Appl. Environ. Microbiol.* 1982; **43**:1070–5.

Charan N. Isolation of Biosurfactant producing organisms from the petroleum contaminated soil in Gujarat. *Int J Pure Appl Biosci* 2017; **5**:893–910.

Chen K, Zhu Q, Qian Y *et al.* Microcalorimetric investigation of the effect of non-ionic surfactant on biodegradation of pyrene by PAH-degrading bacteria *Burkholderia cepacia*. *Ecotoxicol. Environ. Saf.* 2013; **98**:361–7.

Chen SC, Budhraja R, Adrian L *et al.* Novel clades of soil biphenyl degraders revealed by integrating isotope probing, multi-omics, and single-cell analyses. *ISME J* 2021; **15**:3508–21.

Chikere CB, Azubuike CC, Fubara EM. Shift in microbial group during remediation by enhanced natural attenuation (RENA) of a crude oil-impacted soil: a case study of ikarama community, Bayelsa, Nigeria. *3 Biotech* 2017; **7**, DOI: 10.1007/S13205-017-0782-X.

Chikere CB, Fenibo EO. Distribution of PAH-ring hydroxylating dioxygenase genes in bacteria isolated from two illegal oil refining sites in the Niger Delta, Nigeria. *Scientific African* 2018; **1**:e00003.

Chukamnerd A, Singkhamanan K, Chongsuvivatwong V *et al.* Whole-genome analysis of carbapenem-resistant *Acinetobacter baumannii* from clinical isolates in Southern Thailand. *Comput. Struct. Biotechnol. J.* 2022; **20**:545–58.

Cooper DG, Goldenberg BG. Surface-active agents from two *Bacillus* species. *Appl. Environ. Microbiol.* 1987; **53**:224–9.

Cornelissen G, Rigterink H, Ferdinandy MMA *et al.* Rapidly desorbing fractions of PAHs in contaminated sediments as a predictor of the extent of bioremediation. *Environ. Sci. Technol.* 1998; **32**:966–70.

Cosentino S, Voldby Larsen M, Møller Aarestrup F *et al.* PathogenFinder--distinguishing friend from foe using bacterial whole genome sequence data. *PLoS One* 2013; **8**, DOI: 10.1371/JOURNAL.PONE.0077302.

Czarny J, Staninska-Pięta J, Piotrowska-Cyplik A *et al. Acinetobacter* sp. as the key player in diesel oil degrading community exposed to PAHs and heavy metals. *J. Hazard. Mater.* 2020; **383**, DOI: 10.1016/J.JHAZMAT.2019.121168.

Davis JJ, Gerdes S, Olsen GJ *et al.* PATtyFams: Protein families for the microbial genomes in the PATRIC database. *Front. Microbiol.* 2016; **7**:118.

Denome SA, Stanley DC, Olson ES *et al.* Metabolism of dibenzothiophene and naphthalene in *Pseudomonas* strains: Complete DNA sequence of an upper naphthalene catabolic pathway. *J. Bacteriol. Res.* 1993; **175**:6890–901.

Eaton RW, Chapman PJ. Bacterial metabolism of naphthalene: construction and use of recombinant bacteria to study ring cleavage of 1,2-dihydroxynaphthalene and subsequent reactions. *J. Bacteriol. Res.* 1992; **174**:7542–54.

Eze EC, Chenia HY, el Zowalaty ME. Infection and drug resistance dovepress *Acinetobacter baumannii* biofilms: effects of physicochemical factors, virulence, antibiotic resistance determinants, gene regulation, and future antimicrobial treatments. *Infect. Drug Resist.* 2018, DOI: 10.2147/IDR.S169894.

Fondi M, Rizzi E, Emiliani G *et al.* The genome sequence of the hydrocarbon-degrading *Acinetobacter venetianus* VE-C3. *Res. Microbiol.* 2013; **164**:439–49.

Fuchs G, Boll M, Heider J. Microbial degradation of aromatic compounds- From one strategy to four. *Nat. Rev. Microbiol.* 2011; **9**:803–16.

Furlan JPR, de Almeida OGG, de Martinis ECP *et al.* Characterization of an environmental multidrug-resistant *Acinetobacter seifertii* and comparative genomic

analysis reveals co-occurrence of antimicrobial resistance and metal tolerance determinants. *Front. Microbiol.* 2019; **10**, DOI: 10.3389/FMICB.2019.02151.

Ghosal D, Dutta A, Chakraborty J *et al.* Characterization of the metabolic pathway involved in assimilation of acenaphthene in *Acinetobacter* sp. strain AGAT-W. *Res. Microbiol.* 2013; **164**:155–63.

Ghosal D, Ghosh S, Dutta TK *et al.* Current state of knowledge in microbial degradation of polycyclic aromatic hydrocarbons (PAHs): A review. *Front. Microbiol.* 2016; **7**, DOI: 10.3389/fmicb.2016.01369.

Gibson DT, Parales RE. Aromatic hydrocarbon dioxygenases in environmental biotechnology. *Curr. Opin. Biotechnol.* 2000; **11**:236–43.

Giuliani S, Sprovieri M, Frignani M *et al.* Presence and origin of polycyclic aromatic hydrocarbon in sediments of nine coastal lagoons in central Vietnam. *Mar. Pollut. Bull.* 2008; **56**:1504–12.

Goveas LC, Sajankila SP. Effect of yeast extract supplementation on halotolerant biosurfactant production kinetics coupled with degradation of petroleum crude oil by *Acinetobacter baumannii* OCB1 in marine environment. *Bioresour. Technol.* 2020; **11**:100447.

Grund AD, Gunsalus IC. Cloning of genes for naphthalene metabolism in *Pseudomonas putida. J. Bacteriol. Res.* 1983; **156**:89–94.

Guo CL, Zhou HW, Wong YS *et al.* Isolation of PAH-degrading bacteria from mangrove sediments and their biodegradation potential. *Mar. Pollut. Bull.* 2005; **51**:1054–61.

Guo QQ, Ming H, Meng XL *et al*. *Rhodococcus agglutinans* sp. nov., an *Actinobacterium* isolated from a soil sample. *Antonie Van Leeuwenhoek* 2015; **107**:1271–80.

Guo Y, Wu K, Huo X *et al.* Sources, distribution, and toxicity of polycyclic aromatic hydrocarbons. *J Environ Health* 2011; **73**:22–5.

Gupta B, Puri S, Thakur IS *et al.* Enhanced pyrene degradation by a biosurfactant producing *Acinetobacter baumannii* BJ5: Growth kinetics, toxicity and substrate inhibition studies. *Environ. Technol. Innov.* 2020; **19**, DOI: 10.1016/J.ETI.2020.100804.

Habe H, Omori T. Genetics of Polycyclic Aromatic hydrocarbon metabolism in diverse aerobic bacteria. *Biosci. Biotechnol. Biochem.* 2003; **67**:225–43.

Haleyur N, Shahsavari E, Jain SS *et al.* Influence of bioaugmentation and biostimulation on PAH degradation in aged contaminated soils: Response and dynamics of the bacterial community. *J. environ. manag. saf.* 2019; **238**:49–58.

Hatzinger PB, Alexander M. Effect of aging of chemicals in soil on their biodegradability and extractability. *Environ. Sci. Technol.* 1995; **29**:537–45.

Heitkamp MA, Freeman JP, Miller DW *et al.* Pyrene degradation by a *Mycobacterium* sp.: identification of ring oxidation and ring fission products. *Appl. Environ. Microbiol.* 1988; **54**:2556–65.

Hong Sunhee FCE. Is it essential to sequence the entire 16S rRNA gene for bacterial identification? *Eur. Pharm. Rev. Com* 2016:1–13.

Huang R Ying, Tian W Jun, Liu Q *et al.* Enhanced biodegradation of pyrene and indeno(1,2,3-cd)pyrene using bacteria immobilized in cinder beads in estuarine wetlands. *Mar. Pollut. Bull.* 2016; **102**:128–33.

Hussar E, Richards S, Lin ZQ *et al.* Human health risk assessment of 16 priority polycyclic aromatic hydrocarbons in soils of Chattanooga, Tennessee, USA. *Water Air Soil Pollut.* 2012; **223**:5535–48.

Isaac P, Lozada M, Dionisi HM *et al.* Differential expression of the catabolic *nahAc* gene and its effect on PAH degradation in *Pseudomonas* strains isolated from contaminated Patagonian coasts. *Int. Biodeterior. Biodegradation* 2015; **105**:1–6.

Jacob J. The significance of polycyclic aromatic hydrocarbons as environmental carcinogens. *Pure Appl. Chem.* 1996; **68**:301–8.

Jiang Y, Zhang Z, Zhang X. Co-biodegradation of pyrene and other PAHs by the bacterium *Acinetobacter johnsonii*. *Ecotoxicol. Environ. Saf.* 2018; **163**:465–70.

Juhasz AL, Britz ML, Stanley GA. Degradation of high molecular weight polycyclic aromatic hydrocarbons by *Pseudomonas cepacia*. *Biotechnol. Lett. 1996 18:5* 1996; **18**:577–82.

Juhasz AL, Britz ML, Stanley GA. Degradation of fluoranthene, pyrene, benz[a]anthracene and dibenz[a,h]anthracene by *Burkholderia cepacia*. *J. Appl. Microbiol.* 1997; **83**:189–98.

Kanaly RA, Harayama S. Advances in the field of high-molecular-weight polycyclic aromatic hydrocarbon biodegradation by bacteria. *Microb. Biotechnol.* 2010; **3**:136–64.

Kanehisa M, Sato Y, Kawashima M *et al.* KEGG as a reference resource for gene and protein annotation. *Nucleic Acids Res.* 2016; **44**:D457.

Kang YS, Jung J, Jeon CO *et al. Acinetobacter oleivorans* sp. nov. Is capable of adhering to and growing on diesel-oil. *J. Microbiol. 2011 49:1* 2011; **49**:29–34.

Kasai Y, Shindo K, Harayama S *et al.* Molecular characterization and substrate preference of a polycyclic aromatic hydrocarbon dioxygenase from *Cycloclasticus* sp. Strain A5. *Appl. Environ. Microbiol.* 2003; **69**:6688–97.

Kästner M, Breuer-Jammali M, Mahro B. Enumeration and characterization of the soil microflora from hydrocarbon-contaminated soil sites able to mineralize polycyclic aromatic hydrocarbons (PAH). *Appl. Microbiol. Biotechnol. 1994 41:2* 1994; **41**:267–73.

Kirstine W v., Galbally IE. The global atmospheric budget of ethanol revisited. *Atmospheric Chem. Phys.* 2012; **12**:545–55.

Kiyohara H, Torigoe S, Kaida N *et al.* Cloning and characterization of a chromosomal gene cluster, *pah*, that encodes the upper pathway for phenanthrene and naphthalene utilization by *Pseudomonas putida* OUS82. *J. Bacteriol. Res.* 1994; **176**:2439–43.

Kong F Xin, Sun G Dong, Liu Z Pei. Degradation of polycyclic aromatic hydrocarbons in soil mesocosms by microbial/plant bioaugmentation: Performance and mechanism. *Chemosphere* 2018; **198**:83–91.

Kotoky R, Das S, Singha LP *et al.* Biodegradation of Benzo(a)pyrene by biofilm forming and plant growth promoting *Acinetobacter* sp. strain PDB4. *Environ. Technol. Innov.* 2017; **8**:256–68.

Kuppusamy S, Thavamani P, Venkateswarlu K *et al.* Remediation approaches for polycyclic aromatic hydrocarbons (PAHs) contaminated soils: Technological constraints, emerging trends and future directions. *Chemosphere* 2017; **168**:944–68.

Laurie AD, Lloyd-Jones G. The *phn* genes of *Burkholderia* sp. strain RP007 constitute a divergent gene cluster for polycyclic aromatic hydrocarbon catabolism. *J. Bacteriol. Res.* 1999; **181**:531–40.

Lee DW, Lee H, Lee AH *et al.* Microbial community composition and PAHs removal potential of indigenous bacteria in oil contaminated sediment of Taean coast, Korea. *Environ. Pollut.* 2018; **234**:503–12.

Li A, Qu Y, Zhou J *et al.* Enzyme–substrate interaction and characterization of a 2,3-dihydroxybiphenyl 1,2-dioxygenase from *Dyella ginsengisoli* LA-4. *FEMS Microbiol. Lett.* 2009; **292**:231–9.

Li J, Cao J, Wang X *et al. Acinetobacter pittii*, an emerging new multi-drug resistant fish pathogen isolated from diseased blunt snout bream (*Megalobrama amblycephala* Yih) in China. *Appl. Microbiol. Biotechnol.* 2017; **101**:6459–71.

Liang C, Huang Y, Wang H. *pahE*, a functional marker gene for polycyclic aromatic hydrocarbon-degrading bacteria. *Appl. Environ. Microbiol.* 2019; **85**, DOI: 10.1128/AEM.02399-18.

Liebeg EW, Cutright TJ. The investigation of enhanced bioremediation through the addition of macro and micro nutrients in a PAH contaminated soil. *Int. Biodeterior. Biodegradation* 1999; **44**:55–64.

Lindemann S, Nelson WC, Chia N *et al.* PATtyFams: Protein families for the microbial genomes in the PATRIC database. *Front. Microbiol.* | *www.frontiersin.org* 2016; **7**:118.

Liu F, Niu L, Chen H *et al.* Seasonal changes of polycyclic aromatic hydrocarbons in response to hydrology and anthropogenic activities in the Pearl River estuary, China. *Mar. Pollut. Bull.* 2017; **117**:255–63.

Liu F, Yang Q, Hu Y *et al.* Distribution and transportation of polycyclic aromatic hydrocarbons (PAHs) at the humen river mouth in the Pearl River delta and their influencing factors. *Mar. Pollut. Bull.* 2014; **84**:401–10.

Liu Y, Hu H, Zanaroli G *et al.* A *Pseudomonas* sp. strain uniquely degrades PAHs and heterocyclic derivatives via lateral dioxygenation pathways. *J. Hazard. Mater.* 2021; **403**, DOI: 10.1016/J.JHAZMAT.2020.123956.

Lloyd-Jones G, Laurie AD, Hunter DWF *et al.* Analysis of catabolic genes for naphthalene and phenanthrene degradation in contaminated New Zealand soils. *FEMS Microbiol. Ecol.* 1999; **29**:69–79.

Lovanh N, Hunt CS, Alvarez PJJ. Effect of ethanol on BTEX biodegradation kinetics: Aerobic continuous culture experiments. *Water Res.* 2002; **36**:3739–46.

Lu C, Hong Y, Liu J *et al.* A PAH-degrading bacterial community enriched with contaminated agricultural soil and its utility for microbial bioremediation. *Environ. Pollut.* 2019; **251**:773–82.

Ma X, Li X, Liu J *et al.* Soil microbial community succession and interactions during combined plant/white-rot fungus remediation of polycyclic aromatic hydrocarbons. *Sci. Total Environ.* 2021; **752**:142224.

Mallah MA, Changxing L, Mallah MA *et al.* Polycyclic aromatic hydrocarbon and its effects on human health: An overview. *Chemosphere* 2022; **296**, DOI: 10.1016/J.*CHEMOSPHERE*. 2022.133948.

Mehetre GT, Dastager SG, Dharne MS. Biodegradation of mixed polycyclic aromatic hydrocarbons by pure and mixed cultures of biosurfactant producing thermophilic and thermo-tolerant bacteria. *Sci. Total Environ.* 2019; **679**:52–60.

Menn FM, Applegate BM, Sayler GS. NAH plasmid-mediated catabolism of anthracene and phenanthrene to naphthoic acids. *Appl. Environ. Microbiol.* 1993; **59**:1938–42.

Mercadal JPR, Isaac P, Siñeriz F *et al.* Indigo production by *Pseudomonas* sp. J26, a marine naphthalene-degrading strain. *J. Basic Microbiol.* 2010; **50**:290–3.

Meyer S, Moser R, Neef A *et al.* Differential detection of key enzymes of polyaromatic-hydrocarbon-degrading bacteria using PCR and gene probes. *Microbiology (N Y)* 1999; **145**:1731–41.

Mohan SV, Kisa T, Ohkuma T *et al.* Bioremediation technologies for treatment of PAH-contaminated soil and strategies to enhance process efficiency. *Reviews in Environ. Biotechnol. 2006 5:4* 2006; **5**:347–74.

Mojiri A, Zhou JL, Ohashi A *et al.* Comprehensive review of polycyclic aromatic hydrocarbons in water sources, their effects and treatments. *Sci. Total Environ.* 2019; **696**:133971.

Mrozik A, Piotrowska-Seget Z. Bioaugmentation as a strategy for cleaning up of soils contaminated with aromatic compounds. *Microbiol. Res.* 2010; **165**:363–75.

Mueller EJ, Loida PJ, Sligar SG. Twenty-five Years of P450 Research. *Cytochrome P450* 1995:83–124.

Mueller JG, Devereux R, Santavy DL *et al.* Phylogenetic and physiological comparisons of PAH-degrading bacteria from geographically diverse soils. *Antonie Van Leeuwenhoek* 1997; **71**:329–43.

Murray JR, Penning TM. Carcinogenic Polycyclic Aromatic Hydrocarbons. *Comprehensive Toxicology* 2018:87–153.

Neidle EL, Hartnett C, Ornston LN *et al.* Nucleotide sequences of the *Acinetobacter calcoaceticus benABC* genes for benzoate 1,2-dioxygenase reveal evolutionary relationships among multicomponent oxygenases. *J. Bacteriol.* 1991; **173**:5385.

Ohadi M, Dehghannoudeh G, Shakibaie M *et al.* Isolation, characterization, and optimization of biosurfactant production by an oil-degrading *Acinetobacter junii* B6 isolated from an Iranian oil excavation site. *Biocatal. Agric. Biotechnol.* 2017; **12**:1–9.

Ondov BD, Treangen TJ, Melsted P *et al.* Mash: Fast genome and metagenome distance estimation using MinHash. *Genome Biol.* 2016; **17**, DOI: 10.1186/s13059-016-0997-x.

Parales RE, Emig MD, Lynch NA *et al.* Substrate specificities of hybrid naphthalene and 2,4-dinitrotoluene dioxygenase enzyme systems. *J Bacteriol* 1998; **180**:2337–44.

Park H, Min B, Jang Y *et al.* Comprehensive genomic and transcriptomic analysis of polycyclic aromatic hydrocarbon degradation by a mycoremediation fungus, *Dentipellis* sp. KUC8613. *Appl. Microbiol. Biotechnol.* 2019; **103**:8145–55.

Patel AB, Shaikh S, Jain KR *et al.* Polycyclic Aromatic Hydrocarbons: sources, toxicity, and remediation approaches. *Front. Microbiol.* 2020; **11**, DOI: 10.3389/fmicb.2020.562813.

Peng RH, Xiong AS, Xue Y *et al.* Microbial biodegradation of polyaromatic hydrocarbons. *FEMS Microbiol. Rev.* 2008; **32**:927–55.

Pothuluri J v., Evans FE, Heinze TM *et al.* Formation of sulfate and glucoside conjugates of benzo[e]pyrene by *Cunninghamella elegans*. *Appl. Microbiol. Biotechnol.* 1996; **45**:677–83.

Rengarajan T, Rajendran P, Nandakumar N *et al.* Exposure to polycyclic aromatic hydrocarbons with special focus on cancer. *Asian Pac J Trop Biomed* 2015; **5**:182–9.

Resnick SM, Torok DS, Lee K *et al.* Regiospecific and stereoselective hydroxylation of 1-indanone and 2-indanone by naphthalene dioxygenase and toluene dioxygenase. *Appl. Environ. Microbiol.* 1995; **61**:847–847.

Rogers SW. Natural attenuation of polycyclic aromatic hydrocarbon-contaminated sites: Review. *J Hazard Toxic Radioact* Waste 2002; **3**, DOI: 10.1061/(ASCE)1090-025X(2002)6.

Rojo F. Degradation of alkanes by bacteria. *Environ. Microbiol.* 2009; **11**:2477–90.

Roy M. Catabolic Versatility of *Sphingobium* sp. strain PNB capable of degrading structurally diverse aromatic compounds. *J Bioremediat Biodegrad* 2013; **04**, DOI: 10.4172/2155-6199.1000173.

Shah MP. Environmental Bioremediation: A low cost nature's natural biotechnology for environmental clean-up. *J Pet Environ Biotechnol* 2014;**05**, DOI: 10.4172/2157-7463.1000191.

Shankhwar AK, Paliwal R. Fungi in bioremediation of soil: Mycoremediation of PAHs compounds. *J Fungi* Elsevier, 2021, 157–70.

Shao Y, Wang Y, Wu X *et al.* Biodegradation of PAHs by *Acinetobacter* isolated from karst groundwater in a coal-mining area. *Environ. Earth Sci.* 2015; **73**:7479–88.

Simarro R, Gonzá Lez N, Fernando Bautista L *et al.* Biodegradation of high-molecular-weight polycyclic aromatic hydrocarbons by a wood-degrading consortium at low temperatures. *Chemosphere* DOI: 10.1111/1574-6941.12006.

Stanier RY, Palleroni NJ, Doudoroff M. The aerobic *pseudomonads*: a taxonomic study. *J. Gen. Microbiol.* 1966; **43**:159–271.

Stoffels M, Amann R, Ludwig W *et al.* Bacterial community dynamics during start-up of a trickle-bed bioreactor degrading aromatic compounds. *Appl. Environ. Microbiol.* 1998; **64**:930–9.

Takeshita T, Kanaly RA. In vitro DNA/RNA Adductomics to confirm DNA damage caused by benzo[a]pyrene in the hep G2 cell Line. *Front. Chem.* 2019; **7**, DOI: 10.3389/FCHEM.2019.00491.

Takizawa N, Iida T, Sawada T *et al.* Nucleotide sequences and characterization of genes encoding naphthalene upper pathway of *pseudomonas aeruginosa* PaK1 and Pseudomonas putida OUS82. *J. Biosci. Bioeng.* 1999; **87**:721–31.

Thangaraj K, Kapley A, Purohit HJ. Characterization of diverse *Acinetobacter* isolates for utilization of multiple aromatic compounds. *Bioresour. Technol.* 2008; **99**:2488–94.

Vaidya S, Devpura N, Jain K *et al.* Degradation of chrysene by enriched bacterial consortium. *Front. Microbiol.* 2018; **9**, DOI: 10.3389/FMICB.2018.01333.

Volokhov D V., Neverov AA, George J *et al.* Genetic analysis of housekeeping genes of members of the genus *Acholeplasma*: Phylogeny and complementary molecular markers to the 16S rRNA gene. *Mol. Phylogenet. Evol.* 2007; **44**:699–710.

Walter U, Beyer M, Klein J *et al.* Degradation of pyrene by *Rhodococcus* sp. UW1. *Appl. Microbiol. Biotechnol. 1991 34:5* 1991; **34**:671–6.

Wang C, Sun H, Li J *et al.* Enzyme activities during degradation of polycyclic aromatic hydrocarbons by white rot fungus *Phanerochaete chrysosporium* in soils. *Chemosphere* 2009; **77**:733–8.

Wattam AR, Abraham D, Dalay O *et al.* PATRIC, the bacterial bioinformatics database and analysis resource. *Nucleic Acids Res.* 2014; **42**:D581–91.

Weissenfels WD, Beyer M, Klein J. Degradation of phenanthrene, fluorene and fluoranthene by pure bacterial cultures. *Appl. Microbiol. Biotechnol.* 1990; **32**:479–84.

Wick RR, Judd LM, Gorrie CL *et al.* Unicycler: Resolving bacterial genome assemblies from short and long sequencing reads. *PLoS Comput Biol* 2017;**13**, DOI: 10.1371/JOURNAL.PCBI.1005595.

Widada J, Nojiri H, Kasuga K *et al.* Molecular detection and diversity of polycyclic aromatic hydrocarbon-degrading bacteria isolated from geographically diverse sites. *Appl. Microbiol. Biotechnol. 2001 58:2* 2002; **58**:202–9.

Willey JM, Sherwood Linda, Woolverton CJ *et al.* Prescott, Harley, and Klein's microbiology. *J Microbiol. Biol. Educ.* 2008.

Wilson SC, Jones KC. Bioremediation of soil contaminated with polynuclear aromatic hydrocarbons (PAHs): a review. *Environ. Pollut.* 1993; **81**:229–49.

Yang Y, Chen RF, Shiaris MP. Metabolism of naphthalene, fluorene, and phenanthrene: preliminary characterization of a cloned gene cluster from *Pseudomonas putida* NCIB 9816. *J. Bacteriol.* 1994; **176**:2158.

Ye D, Akmal Siddiqi M, Maccubbin AE *et al.* Degradation of polynuclear aromatic hydrocarbons by *Sphingomonas paucimobilis*. *Environ. Sci. Technol.* 1996; **30**:136–42.

Yen KM, Gunsalus IC. Plasmid gene organization: naphthalene/salicylate oxidation. *PNAS USA* 1982; **79**:874–8.

Zhan Y, Yan Y, Zhang W *et al.* Comparative analysis of the complete genome of an *Acinetobacter calcoaceticus* strain adapted to a phenol-polluted environment. *Res. Microbiol.* 2012; **163**:36–43.

Zhou H, Huang X, Liang Y *et al.* Enhanced bioremediation of hydraulic fracturing flowback and produced water using an indigenous biosurfactant-producing bacteria *Acinetobacter* sp. Y2. *Chem. Eng. J.* 2020; **397**, DOI: 10.1016/J.CEJ.2020.125348.

Zita A, Hermansson M. Determination of bacterial cell surface hydrophobicity of single cells in cultures and in wastewater *in situ*. *FEMS Microbiol. Lett.* 2006; **152**:299–306.

BIOGRAPHICAL SKETCH

Name of Author: Gunn Emilie Berge

Graduate and Undergraduate Schools Attended:

University of South Alabama, Mobile, Alabama

University of South Alabama, Mobile, Alabama

Degrees Awarded:

Master of Science in Environmental Toxicology, 2022, Mobile, Alabama

Bachelor of Science in Biology, 2020, Mobile, Alabama

Awards and Honors:

Zymo Research Impact Initiative Grant (2022)

Graduate Research Assistant (2020-2022)

Alabama, Graduate Student Activities Enhancement Award Program (2021)

Sun Belt All-Conference Performance (2017, 2018, 2019, 2020, 2021)

2x Second Team All-American (2018, 2019)

Academic All-American (2019)

Female Student-Athlete of the Year (2019)

Freshman Scholar-Athlete of the Year (2017)